

2013

A Study of Nonlinear Dynamics in Mathematical Biology

Joseph Ferrara
University of North Florida

Suggested Citation

Ferrara, Joseph, "A Study of Nonlinear Dynamics in Mathematical Biology" (2013). *UNF Graduate Theses and Dissertations*. 448.
<https://digitalcommons.unf.edu/etd/448>

This Master's Thesis is brought to you for free and open access by the Student Scholarship at UNF Digital Commons. It has been accepted for inclusion in UNF Graduate Theses and Dissertations by an authorized administrator of UNF Digital Commons. For more information, please contact [Digital Projects](#).

© 2013 All Rights Reserved

A STUDY OF NONLINEAR DYNAMICS IN MATHEMATICAL BIOLOGY

by

Joseph Albert Ferrara

A thesis submitted to the Department of Mathematics and Statistics
in partial fulfillment of the requirements for the degree of

Master of Science in Mathematical Sciences

UNIVERSITY OF NORTH FLORIDA
COLLEGE OF ARTS AND SCIENCES

August, 2013

Certificate of Approval

The thesis of Joseph Albert Ferrara is approved:

(Date)

Dr. Mahbubur Rahman, Thesis Advisor

Dr. Adel Boules, Committee Member

Dr. Ognjen Milatovic, Committee Member

Accepted for the Department of Mathematics and Statistics:

Dr. Scott Hochwald, Chair

Accepted for the College of Arts and Sciences:

Dr. Barbara Hetrick, Dean

Accepted for the University:

Dr. Len Roberson, Dean of the Graduate School

Acknowledgements

First and foremost, I would like to thank my advisor Dr. Mahbubur Rahman for the unending and invaluable support he has provided me over the past few months. Were it not for his guidance, encouragement, and patience this process would have been infinitely more difficult.

I would also like to thank Dr. Ognjen Milatovic and Dr. Adel Boules for taking the time to share their thoughts with Dr. Rahman and myself, and for serving on my thesis committee.

I also owe many thanks to all of the faculty in our mathematics department here at the University of North Florida who have served to share the breadth of their knowledge with me, and groom me as a thinker and as a person.

I finally would like to thank my dog, Smokey Bear, for his companionship during this process; for on many a late night he reminded me that sometimes inspiration comes from just sitting around and doing nothing.

Table of Contents

Acknowledgements	iii
Table of Contents	iv
Abstract	v
Chapter 1. Introduction	1
Chapter 2. Background Material	3
2.1 The Dynamical System	3
2.2 Equilibria, Linearization, and Stability Analysis	4
2.3 Periodic Solutions and Limit Cycles	11
2.4 The Hopf-Bifurcation	23
2.5 Modeling Interacting Populations	27
Chapter 3. A Mathematical Modeling of Tumor Growth	34
3.1 Model 1 - Analysis of the Effector/Tumor Cell Interaction	34
3.2 Model 2- Inclusion of IL-2	40
Chapter 4. Concluding Remarks	54
Chapter 5. Appendix	56
5.1 Nondimensionalization and Scaling Techniques	56
5.2 Michaelis-Menten Kinetics	59
5.3 More about the Poincare-Bendixson Theorem	60
5.4 Elementary Bifurcations	61
Bibliography	65

Abstract

We first discuss some fundamental results such as equilibria, linearization, and stability of nonlinear dynamical systems arising in mathematical modeling. Next we study the dynamics in planar systems such as limit cycles, the Poincaré-Bendixson theorem, and some of its useful consequences. We then study the interaction between two and three different cell populations, and perform stability and bifurcation analysis on the systems. We also analyze the impact of immunotherapy on the tumor cell population numerically.

CHAPTER 1

Introduction

To begin studying nonlinear dynamical systems requires a complete understanding of how linear systems behave. The books [3, 4, 5, 8, 19, 22] all provide a full development of linear theory. The essential results of linear theory include the existence and uniqueness of solutions, the behavior of equilibrium points based on eigenvalue analysis, and the extension of linear systems into \mathbb{R}^n through the structure of linear algebra and the matrix exponential. The reason for the emphasis on linear theory is that locally, in the neighborhood of an equilibrium and under certain conditions, nonlinear systems behave identically to linear systems. Thus we can often characterize the qualitative behavior of a nonlinear system by analyzing the corresponding locally linear system at the equilibrium points, and piecing the results together. The importance of this cannot be understated, since explicit solutions for nonlinear systems are most often extremely difficult or impossible to determine.

Dynamical systems play an important role in determining the fate of many interacting systems. They are used to model a variety of phenomena found in the physical, financial, and biological realms. In [12] there is a rich development of nonlinear dynamical systems, and it is the primary source we follow for much of our paper. A continuation of [12] is found in [18] which applies the dynamical system to manifolds and thus generates even more theoretical results. Manifold theory will not play a role in this paper since we are primarily interested in the interacting populations model which does not require the notion of a manifold. In [6, 9] there is a rich number of biological problems, and the general theory we develop in this paper has been tailored to the needs of such problems. A more advanced look at the development of dynamical system models and theory can be found in [10, 16, 23].

In Chapter 2 we give some background material on the subject which provides the framework needed to study a nonlinear dynamical system regardless of the phenomenon being considered. In Chapter 3 we study the models in [14] and [13], and analyze the details of the development and dynamics of the models mathematically and numerically. We also determine the possible fates of these systems, and add the treatment described in [20] to the model. In Chapter 4 we make some concluding remarks, and Chapter 5 is the Appendix which contains a variety of topics necessary to the cohesion of the preceding materials.

CHAPTER 2

Background Material

2.1. The Dynamical System

A dynamical system is a way of describing the properties of a physical system through time. Examples of this include the space of states S of a system such as a particle moving through space as time goes on, and the interaction among n different populations competing for resources. We often define dynamical systems on a Euclidean space or open subsets of a Euclidean space. Given a dynamical system on S we are able to precisely locate where a particle is initially, call it x_0 or at one unit of time later, call it x_1 or at one unit of time prior, call it x_{-1} . By considering all such positions we can extrapolate them in a continuous way to fill up all real numbers and obtain the solution $x(t) = x_t$ for any given $t \in \mathbb{R}$.

The solution of a dynamical system, a function of time that satisfies initial conditions is called the *flow* of the system. We assume the map $\phi : \mathbb{R} \times S \rightarrow S$ defined by $\phi(t, x) = x_t$ is at least continuously differentiable in t . The flow has an inverse ϕ_{-t} and we denote $\phi_0(x)$ to be the identity and furthermore the composition of two flows exists as $\phi_t(\phi_s(x)) = \phi_{t+s}(x)$. This leads to the following definition of a dynamical system.

DEFINITION 1. A dynamical system is a C^1 map $\phi : \mathbb{R} \times S \rightarrow S$ where S is an open set of a Euclidean space and writing $\phi(t, x) = \phi_t(x)$, the map $\phi_t : S \rightarrow S$ satisfies,

- (i) $\phi_0 : S \rightarrow S$ is the identity,
- (ii) The composition $\phi_t \circ \phi_s = \phi_{t+s}$ for each $t, s \in \mathbb{R}$.

Throughout this paper we let E denote a vector space with a norm $\|\cdot\|$, and $W \subset E$ be an open set in E , and let $f : W \rightarrow E$ be a continuous map. A solution to the differential equation,

$$(2.1.1) \quad x' = f(x)$$

refers to a differentiable function,

$$u : J \rightarrow W$$

defined on an interval $J \subset \mathbb{R}$ such that $\forall t \in J$ where J is an open, closed, or half-open interval on \mathbb{R} ,

$$u'(t) = f(u(t)).$$

It can be shown that every dynamical system gives rise to a differential equation, and that every differential equation gives rise to a dynamical system.

2.2. Equilibria, Linearization, and Stability Analysis

In this section we analyze the nonlinear system (2.1.1) by determining its equilibrium points, and using linearization techniques to describe the behavior of the system near the equilibria.

Some of the most important types of solutions are ones in which the system (2.1.1) is not changing. Such solutions are called equilibrium points, and they are defined below.

DEFINITION 2. An *equilibrium point* $\bar{x} \in W$ of the system (2.1.1) is a solution that satisfies $f(\bar{x}) = 0$ for all t .

The stability of an equilibrium point of (2.1.1) is an important notion whereby the long-term behavior of a solution may be determined through stability analysis of the

equilibrium points. An equilibrium point \bar{x} with initial condition \bar{x}_0 is called stable if all solutions that begin near \bar{x} stay near \bar{x} for all $t \geq 0$. We say that the equilibrium point \bar{x} is asymptotically stable if all nearby solutions not only stay nearby, but also tend toward \bar{x} .

The study of equilibria and their stability plays an important role in determining the usefulness of a mathematical model with respect to its corresponding physical or biological system. This is especially true for a system where the initial conditions are not exactly known. The three different types of equilibria are defined below.

DEFINITION 3. Suppose $\bar{x} \in W$ is an equilibrium of (2.1.1). Then \bar{x} is a *stable* equilibrium if for every neighborhood U of \bar{x} there is a neighborhood U_1 of \bar{x} in U such that every solution x_t with x_0 in U_1 is defined and in U for all $t > 0$.

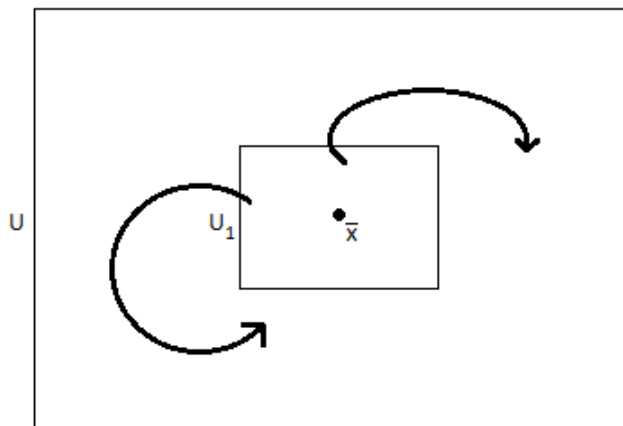


FIGURE 2.2.1. A stable equilibrium point.

The definition for asymptotic stability is obtained by adding an additional condition to Definition 3.

DEFINITION 4. We say that $\bar{x} \in W$ is *asymptotically stable* if in addition to the properties described in Definition 3 it also has the property that $\lim_{t \rightarrow \infty} x(t) = \bar{x}$.

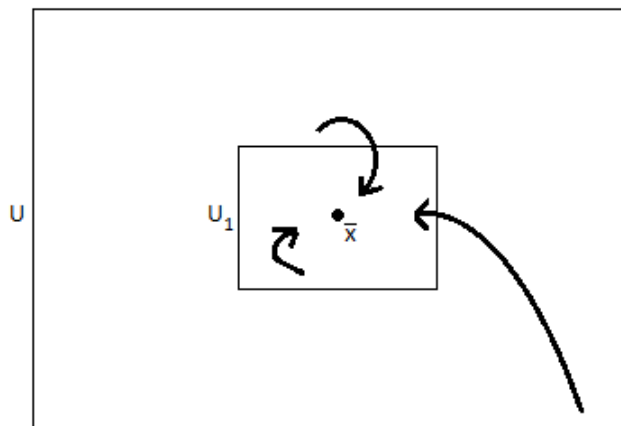


FIGURE 2.2.2. An asymptotically stable equilibrium point.

The definition of an unstable equilibrium point is as follows.

DEFINITION 5. An equilibrium point $\bar{x} \in W$ that is not stable or asymptotically stable is called *unstable*. This means there is a neighborhood U of \bar{x} such that for every neighborhood U_1 of \bar{x} in U , there is at least one solution x_t starting at $x_0 \in U_1$, which does not lie entirely in U .

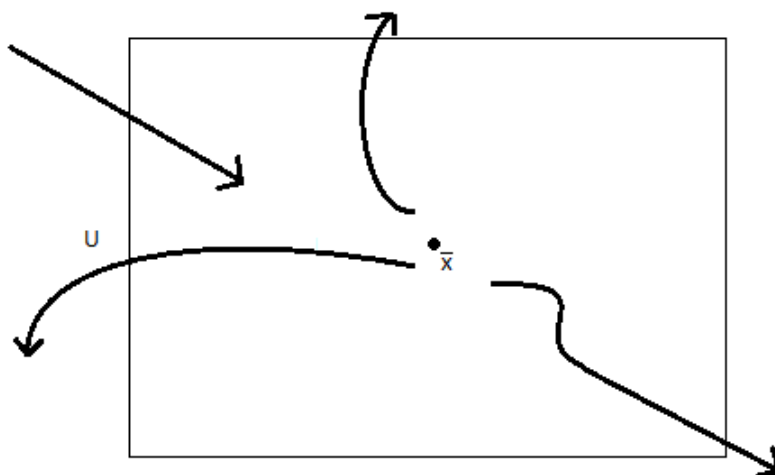


FIGURE 2.2.3. An unstable equilibrium point.

2.2.1. Stability.

DEFINITION 6. An equilibrium point \bar{x} is *hyperbolic* if none of the eigenvalues of the matrix $D(f(\bar{x}))$ have zero real part.

It is shown that the local behavior of nonlinear systems near a hyperbolic equilibrium point \bar{x} is qualitatively determined by the behavior of the linear system,

$$x' = Ax$$

for the matrix $A = D(f(\bar{x}))$ which is a linear operator represented by the $n \times n$ matrix of partial derivatives,

$$\frac{\partial}{\partial x_j} (f_i(x_1, \dots, x_n)) \quad \text{for } i, j = 1, 2, \dots, n$$

near the origin. The linear function $Ax = D(f(\bar{x}))x$ is called the linear part of $f(x)$ at \bar{x} . As long as $D(f(\bar{x}))$ has no zero or pure imaginary eigenvalues, then this linear part will approximate the local behavior of the nonlinear system near the equilibrium point. A detailed derivation of this linearization idea is given in Section 2.5, where we define the Jacobian which is a matrix that represents the linearized part of the nonlinear system near an equilibrium point.

DEFINITION 7. An equilibrium point \bar{x} of (2.1.1) is called a *sink* if all of the eigenvalues of the matrix $D(f(\bar{x}))$ have negative real part; it is called a *source* if all of the eigenvalues of $D(f(\bar{x}))$ have positive real part; and it is called a *saddle* if it is a hyperbolic equilibrium point and $D(f(\bar{x}))$ has at least one eigenvalues with a positive real part and at least one with a negative real part.

The corresponding matrix evaluated at an equilibrium point \bar{x} will yield eigenvalues, and it is the eigenvalues that determine the stability properties of the corresponding equilibrium point. This idea is expressed in the following theorems.

THEOREM 8. *If all eigenvalues of $D(f(\bar{x}))$ of the system (2.1.1) have negative real part, then the equilibrium \bar{x} is asymptotically stable.*

The proof of Theorem 8 follows after we discuss Theorem 9 and Liapunov's Theorem. The following theorem provides an important stability result that states for every positive equilibrium point none of the eigenvalues of $D(f(\bar{x}))$ have positive real part.

THEOREM 9. *Let $W \subset E$ be open and $f : W \rightarrow E$ be continuously differentiable. If $f(\bar{x}) = 0$ and \bar{x} is a stable equilibrium point of $x' = f(x)$ then no eigenvalue of $D(f(\bar{x}))$ has positive real part.*

PROOF. See [12, pg.187] for the proof. □

A useful theoretical result was discovered by the Russian mathematician and engineer Liapunov. The result provides a criteria whereby if a certain function V behaves in a certain way, then the stability of the corresponding equilibrium point can be determined. This idea is presented in Theorem 10, but first we develop some notation needed to express the theorem.

Let $V : U \rightarrow \mathbb{R}$ be a differentiable function defined in a neighborhood $U \subset W$ of \bar{x} . We denote by $V' : U \rightarrow \mathbb{R}$ the function defined by,

$$V'(x) = DV(x)(f(x)),$$

where $DV(x)$ is the differential operator applied to the vector $f(x)$. Suppose $\phi_t(x)$ is a solution to 2.1.1 with $E = \mathbb{R}^n$ at $t = 0$ passing through x then,

$$V'(x) = \frac{d}{dt} V(\phi_t(x))|_{t=0}$$

by the chain rule. If V' is negative notice that V then decreases along the solution through x .

THEOREM 10 (Liapunov's Theorem). *Let $\bar{x} \in W$ be an equilibrium for $x' = f(x)$ where $f : W \rightarrow \mathbb{R}^n$ is a C^1 map on an open set $W \subset \mathbb{R}^n$. Let $V : U \rightarrow \mathbb{R}$ be a continuous function defined on a neighborhood $U \subset W$ of \bar{x} , differentiable on $U - \bar{x}$, such that,*

$$(i) \ V(\bar{x}) = 0 \text{ and } V(x) > 0 \text{ if } x \neq \bar{x},$$

$$(ii) \ V' \leq 0 \text{ in } U - \bar{x}.$$

Then \bar{x} is stable. Furthermore, if also,

$$(iii) \ V' < 0 \text{ in } U - \bar{x},$$

then \bar{x} is asymptotically stable.

PROOF. See [12, pg.193] for the proof. □

EXAMPLE 11. Consider the planar system,

$$x_1' = -x_1 - x_1x_2^2$$

$$x_2' = -x_2 - x_1^2x_2$$

Then the function $V = x_1^2 + x_2^2$ yields,

$$V' = -2x_1^2(1 + x_2^2) - 2x_2^2(1 + x_1^2)$$

$$= -2(x_1^2 + x_2^2 + 2x_1^2x_2^2)$$

$$< 0$$

Since $x_1^2 + x_2^2 + 2x_1^2x_2^2 > 0$ for all $(x_1, x_2) \in \mathbb{R}^2$ and $V'(0, 0) = 0$ only for the equilibrium point, then it follows from Theorem 9 that the equilibrium point $\bar{x} = (0, 0)$ is asymptotically stable.

Notice that for an asymptotically stable equilibrium point the quantity $\|x - \bar{x}\| \rightarrow 0$ as $t \rightarrow \infty$. Liapunov realized that the norm need not be the only quantity that tends

to zero as the solution gets closer and closer to the equilibrium point, namely he found that the above conditions on a devised function V would also guarantee stability.

We now proceed with the proof of Theorem 8.

PROOF. Let $\bar{x} \in W$ be an equilibrium for $x' = f(x)$ where $f : W \rightarrow \mathbb{R}^n$ is a C^1 map on an open set $W \subset \mathbb{R}^n$. Let $y = x - \bar{x}$ translate the fixed point to the origin so that we obtain,

$$y' = f(y + \bar{x}), \quad y \in \mathbb{R}^n$$

Using the Taylor expansion we obtain,

$$(2.2.1) \quad y' = D(f(\bar{x})y) + R(y)$$

with $R(y) \equiv \mathcal{O}(|y^2|)$, where $R(y) \equiv \mathcal{O}(|y^2|)$ if and only if there exists $K > 0 \in \mathbb{R}$ and $y_0 \in \mathbb{R}$ such that $|R(y)| \leq K|y^2|$ for all $y > y_0$.

Let $y = \epsilon u$ where $0 < \epsilon < 1$, which implies that for a small ϵ we have a small y vector.

Thus (2.2.1) becomes,

$$u' = D(f(\bar{x})u) + \bar{R}(u, \epsilon)$$

where $\bar{R}(u, \epsilon) = \frac{R(\epsilon u)}{\epsilon}$. Let $\bar{R}(u, 0) \equiv \lim_{\epsilon \rightarrow \infty} \bar{R}(u, \epsilon) \rightarrow 0$ since $R(y) \equiv \mathcal{O}(|y^2|)$.

Let the Liapunov function be defined as,

$$V(u) = \frac{1}{2} |u|^2.$$

it then follows that,

$$\begin{aligned} V'(u) &= \nabla V(u) \cdot u' \\ &= (u \cdot D(f(\bar{x})u)) + (u \cdot \bar{R}(u, \epsilon)). \end{aligned}$$

Since all of the eigenvalues of $D(f(\bar{x})u)$ have negative real part,

$$u \cdot D(f(\bar{x})u) < k|u|^2 < 0$$

for some real number k and all u . Hence for ϵ small enough $V'(u)$ is strictly negative, and thus the fixed point \bar{x} is asymptotically stable. \square

As we have seen, the stability of an equilibrium point of a nonlinear system can often be determined by analyzing the eigenvalues of the corresponding linearized system. However, not all equilibrium points exhibit this type of limiting behavior, in fact there often exist periodic solutions. In the next section we develop tools used to understand some of the dynamics that arise as a result of these periodic solutions, and we prove a very important classical result for planar dynamical systems.

2.3. Periodic Solutions and Limit Cycles

In the preceding section we analyzed the behavior of solutions starting near an equilibrium point. For first order differential equations this was enough to describe the behavior of all solutions, as every solution is either unbounded or approaches an equilibrium point. As we will see, solutions to second order differential equations yield other possible limiting behaviors. Consequently, we must consider what happens to a solution that does not begin near equilibria. Such systems often arise in models of interacting populations.

We still consider a dynamical system on an open set W in a vector space E , that is we define ϕ_t on a C^1 vector field $f : W \rightarrow E$. We now develop a handful of results needed to prove the main results of Subsections 2.3.4 and 2.3.5.

Invariance refers to a certain mathematical property that is maintained after a transformation is applied to it. For example, the degree of a polynomial $P_n(x)$ is not invariant under the derivative operator, as the degree is reduced after the transformation is applied. The invariance of a dynamical system is essentially a statement of boundedness and existence of solutions in a certain set, and is defined below.

DEFINITION 12. A set A in the domain W of a dynamical system is *invariant* if for every $x \in A$, $\phi_t(x)$ is defined and in A for all $t \in \mathbb{R}$. A system is said to be *positively invariant* if the definition of invariance is met for all $t \geq 0$.

An equilibrium point is a simple example of an invariant set. Also a periodic orbit, which will be discussed shortly, is an example of an invariant set because the set of all points that start on a periodic orbit will always be defined and remain on the orbit for all time.

2.3.1. Limit Sets. For planar dynamical systems limit sets are fairly simple, for example every equilibrium point is its own α and ω -limit set, and every asymptotically stable solution is also an ω -limit set for every point in its basin. These ideas are defined below.

DEFINITION 13. Let $y \in \mathbb{R}^n$ be an ω -*limit point* for the solution through x if there is a sequence $t_n \rightarrow \infty$ such that $\lim_{n \rightarrow \infty} \phi_{t_n}(x) = y$. The set of all ω -*limit points* of the solution through x is the ω -*limit set* of x and is denoted by $L_\omega(x)$. The α -*limit set* is designed similarly, except $t_n \rightarrow -\infty$ and it is denoted by $L_\alpha(x)$.

EXAMPLE 14. Consider the second-order differential equation,

$$x'' = -x.$$

A solution is $x_t = \sin(t)$. An ω -limit point is such that for a sequence t_n we have as $t_n \rightarrow \infty$ that $x_{t_n} = r$ where $r \in \mathbb{R}$. Such a sequence exists for $r \in [-1, 1]$ and hence $L_\omega(x) = [-1, 1]$. Furthermore, since $\sin(t)$ is periodic one can easily find sequences that always yield the same values as $t_n \rightarrow \infty$.

Some facts regarding limit sets are recorded in the following proposition.

PROPOSITION 15. (i) *If x and z are on the same solution, then $L_\omega(x) = L_\omega(z)$ and $L_\alpha(x) = L_\alpha(z)$.*

(ii) If D is a closed positively [negatively] invariant set and $z \in D$, then $L_\omega(z) \subset D$ [$L_\alpha(z) \subset D$].

(iii) A closed invariant set, in particular a limit set, contains the α -limit and ω -limit sets of every point in it.

PROOF. (i) Suppose that $y \in L_\omega(x)$, and $\phi_s(x) = z$, in other words for some time s the flow at x is equivalent to z . If $\phi_{t_n}(x) \rightarrow y$, then we can shift z to x by $\phi_{t_n-s}(z) = \phi_{t_n}(x) \rightarrow y$. Hence, $y \in L_\omega(z)$ also.

(ii) If $\phi_{t_n}(z) \rightarrow y \in L_\omega(z)$ as $t_n \rightarrow \infty$, then we have $t_n \geq 0$ for n large enough so that $\phi_{t_n}(z) \in D$. Therefore, $y \in D$ since D is a closed set.

(iii) Follows immediately from (ii). □

2.3.2. Local Sections and Flow Boxes. The proof of the Poincaré-Bendixson Theorem in this paper requires the concepts of local sections and flow boxes, which we define in this section. As above, we still consider the flow ϕ_t of the C^1 vector field $f : W \rightarrow E$ and suppose the origin $0 \in E$ belongs to W .

DEFINITION 16. A local section at 0 of f is an open set S containing 0 in the hyperplane $H \subset E$ which is transverse to f .

The hyperplane H of E is a linear subspace of E whose dimension is one less than E . To say that $S \subset H$ is transverse to f means that $f(x) \notin H \ \forall x \in S$. Particularly we mean that $f(x) \neq 0$ for $x \in S$.

The local section is devised so that we can consider the flow of a solution in a neighborhood of 0 . A flow box provides a complete description of a flow in a neighborhood of a nonequilibrium point of any flow by choosing a special set of coordinates. The idea is that points move in parallel straight lines at constant speed.

DEFINITION 17. Let U and V be open sets of vector spaces. Then a *diffeomorphism* $\Psi : U \rightarrow V$, is a differentiable map from one open set of a vector space to another with a differentiable inverse.

A flow box is a special diffeomorphism defined as follows.

DEFINITION 18. Let N be a neighborhood of $(0, 0)$ in $\mathbb{R} \times H$ and let h be a neighborhood of 0 in W . Then a *flow box* is a diffeomorphism,

$$\Psi : N \rightarrow W$$

that transforms the vector field $f : W \rightarrow E$ into the constant vector field $(1, 0)$ on $\mathbb{R} \times H$. The flow of f is thereby converted to a simple flow on $\mathbb{R} \times H$,

$$\psi_s(t, y) = (t + s, y).$$

The map Ψ is defined by,

$$\Psi(t, y) = \phi_t(y)$$

for (t, y) in a sufficiently small neighborhood of $(0, 0)$ in $\mathbb{R} \times H$.

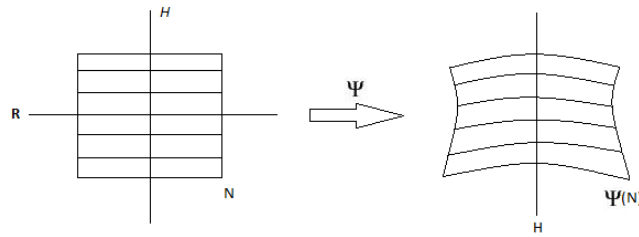


FIGURE 2.3.1. Diagram of the flow box.

A flow box can be defined around any nonequilibrium point x_0 by redefining $f(x)$ by $f(x - x_0)$ which converts the point to 0 .

PROPOSITION 19. Let S be a local section at 0 as above, and suppose $\phi_{t_0}(z_0) = 0$. Then there is an open set $U \subset W$ containing z_0 and a unique C^1 map $\tau : U \rightarrow \mathbb{R}$ such that $\tau(z_0) = t_0$ and,

$$\phi_{\tau(x)}(x) \in S$$

for all $x \in U$.

PROOF. Let $h : E \rightarrow \mathbb{R}$ be a linear map whose kernel H is the hyperplane containing S . Then by definition we have $h(f(0)) \neq 0$. The function,

$$G(x, t) = h\phi_t(x)$$

is C^1 and,

$$\frac{dG}{dt}(z_0, t_0) = h(f(0)) \neq 0.$$

By the implicit function theorem there must exist a unique C^1 map $x \rightarrow \tau(x) \in \mathbb{R}$ defined on a neighborhood U_1 of z_0 in W such that $\tau(z_0) = t_0$ and $G(x, \tau(x)) \equiv 0$. Thus, $\phi_{\tau(x)}(x) \in H$ and for $U \subset U_1$ in a sufficiently small neighborhood of z_0 it follows that $\phi_{\tau(x)} \in S$. \square

2.3.3. Monotone Sequences in the Plane. Let x_0, x_1, x_2, \dots be a finite or infinite sequence of distinct points on the solution curve $C = \{\phi_t(x_0) \mid 0 \leq t \leq \alpha\}$ which is in the plane. The solution is monotone if $\phi_{t_n}(x_0) = x_n$ with $0 \leq t_1 < \dots \leq \alpha$.

Let y_0, y_1, y_2, \dots be a finite or infinite sequence of points on a line segment I in \mathbb{R}^2 . The sequence is monotone along I if the vector $y_n - y_0$ is a scalar multiple $\lambda_n(y_1 - y_0)$ with $1 < \lambda_2 < \lambda_3 < \dots$ $n = 2, 3, \dots$. In other words, $y_{n-1} < y_n < y_{n+1}$ for the ordering along I and $n = 1, 2, \dots$.

For a local section it is impossible for a sequence of points to be monotone along the solution curve but not along the segment I , which is the essence of the following proposition. Notationally we replace the interval I with the local section S .

PROPOSITION 20. *Let S be a local section of a C^1 planar dynamical system and let y_0, y_1, y_2, \dots be a sequence of distinct points of S that lie on the same solution curve C . If the sequence is monotone along C , then it is also monotone along S .*

PROOF. Consider the points y_0, y_1 , and y_2 . Let γ be the simple closed curve made up of the part B of C between y_0 and y_1 and the segment $T \subset S$ between y_0 and y_1 . Let D be the region bounded by γ . Without loss of generality assume the solution of y_1 leaves D at y_1 , where a similar argument follows as it enters instead. Since T is a part of the local section the solution leaves D at every point in T .

It follows that the complement of D is positively invariant, since no solution can enter D at a point of T , and it can never cross B by uniqueness of solutions. Therefore we have, $\phi_t(y_1) \in \mathbb{R}^2 - D$ for all $t > 0$, and specifically we have, $y_2 \in S - T$.

The set $S - T$ can be represented by two half open intervals, I_0 and I_1 with y_0 an endpoint of I_0 and y_1 and endpoint of I_1 . For $\epsilon > 0$ and small enough an arc can be drawn from a point $\phi_\epsilon(y_1)$ to a point I_1 , without crossing γ , and so we can conclude that I_1 is outside D . Thus y_1 is between y_0 and y_2 in I which proves the proposition. The main idea of the argument is illustrated in Figure 2.3.2 below. \square

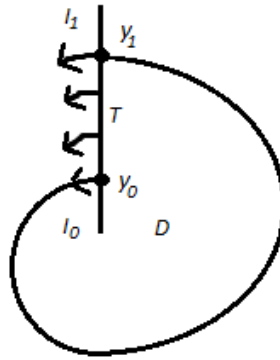


FIGURE 2.3.2. Diagram for Proposition 20.

PROPOSITION 21. *Let $y \in L_\omega(x) \cup L_\alpha(x)$. Then the solution of y crosses any local section at not more than one point.*

PROOF. Suppose y_1 and y_2 are distinct points on the solution of y and S is a local section containing y_1 and y_2 . Without loss of generality suppose $y \in L_\omega(x)$. Then $y_k \in L_\omega(x)$ for $k = 1, 2$. Let $F_{(1)}$ and $F_{(2)}$ be flow boxes at y_k defined by intervals

for all $y \in \Gamma$, $n = 0, \pm 1, \pm 2, \dots$

We now have the tools needed to prove the Poincaré-Bendixson Theorem. As mentioned above the proof requires the Jordan Curve Theorem, which we will assume to be true. The theorem allows us to divide the plane into two components, an “inside” and an “outside”. It is this simple, yet unique to the plane characteristic that allows us to prove the Poincaré-Bendixson theorem, and also the reason the theorem cannot be extended beyond the plane.

THEOREM 22 (The Poincaré-Bendixson Theorem). *A nonempty compact limit set of a C^1 planar dynamical system, which contains no equilibrium point, is a closed orbit.*

PROOF. Without loss of generality we will prove this for ω -limit sets, however the case for α -limit sets is similar. Assume $L_\omega(x)$ is compact and let $y \in L_\omega(x)$. From (ii) of Proposition 15 we know that since y belongs to the compact invariant set $L_\omega(x)$, then $L_\omega(y)$ is a nonempty subset of $L_\omega(x)$.

Let $z \in L_\omega(y)$, S be a local section at z , and F be a flow box neighborhood of z about an open interval J , $z \in J \subset S$. By Proposition 21 we know the solution of y meets S at exactly one point. However, there is a sequence $t_n \rightarrow \infty$ such that $\phi_{t_n}(y) \rightarrow z$, and thus infinitely many $\phi_{t_n}(y)$ belong to F . Thus we can find $r, s \in \mathbb{R}$ such that for $r > s$ and,

$$\phi_r(y) \in S \cap F, \quad \phi_s(y) \in S \cap F.$$

It then follows that $\phi_r(y) = \phi_s(y)$ and so $\phi_{r-s}(y) = y$ and $r - s > 0$. Since $L_\omega(x)$ contains no equilibrium, y belongs to a closed orbit.

Now we must show that if Γ is a closed orbit in $L_\omega(x)$ then $\Gamma = L_\omega(x)$ by proving that,

$$\lim_{t \rightarrow \infty} d(\phi_t(x), \Gamma) = 0$$

where $d(\phi_t(x), \Gamma)$ is the distance from $\phi_t(x)$ to the compact set Γ .

Let S be a local section at $z \in \Gamma$, sufficiently small such that $S \cap \Gamma = z$. By looking at a flow box F_ϵ near z we see that there is a sequence $t_0 < t_1 < t_2 \cdots$ such that,

$$\phi_{t_n}(x) \in S,$$

$$\phi_{t_n} \rightarrow z,$$

$$\phi_t(z) \notin S \quad \text{for} \quad t_{n-1} < t < t_n, \quad n = 1, 2, \dots$$

Let $x_n = \phi_{t_n}(x)$. By Proposition 20 we know that $x_n \rightarrow z$ monotonically in S . Thus there must exist an upper bound for the set of positive numbers $t_{n+1} - t_n$. Suppose $\phi_\lambda(z) = z$, $\lambda > 0$. Then for x_n close enough to z we have $\phi_\lambda(x_n) \in F_\epsilon$ and hence,

$$\phi_{\lambda+t}(x_n) \in S$$

for some $t \in [-\epsilon, \epsilon]$. Thus,

$$t_{n+1} - t_n \leq \lambda + \epsilon.$$

Let $\beta > 0$. Then by properties of norms and continuity there exists $\delta > 0$ such that if $\|x_n - u\| < \delta$ and $|t| \leq \lambda + \epsilon$ then,

$$\|\phi(x_n) - \phi_t(u)\| < \beta.$$

Let n_0 be large enough such that $\|x_n - z\| < \delta$ for all $n \geq n_0$. Then,

$$\|\phi(x_n) - \phi_t(z)\| < \beta$$

if $|t| \leq \lambda + \epsilon$ and $n \geq n_0$. Now let $t \geq t_{n_0}$ and let $n \geq n_0$ be such that,

$$t_n \leq t \leq t_{n+1}.$$

It follows that,

$$\begin{aligned} d(\phi_t(x), \Gamma) &\leq \|\phi_t(x) - \phi_{t-t_n}(z)\| \\ &= \|\phi_{t-t_n}(x_n) - \phi_{t-t_n}(z)\| \\ &< \beta \end{aligned}$$

since $|t - t_n| \leq \lambda + \epsilon$, which completes the proof. \square

2.3.5. Consequences of The Poincaré-Bendixson Theorem. The following results are still for planar dynamics.

DEFINITION 23. A *limit cycle* is a closed orbit Γ such that $\Gamma \subset L_\omega(x)$ or $\Gamma \subset L_\alpha(x)$ for some $x \notin \Gamma$. The former is called an ω -limit cycle and the latter an α -limit cycle.

Limit cycles are special periodic solutions where something like one-sided or possibly two-sided stability exists. For example, a center in a linear system is not a limit cycle because neighboring initial conditions will not tend to the closed orbit, instead they maintain their own orbit.

A consequence of this one- or two-sided stability is as follows.

PROPOSITION 24. *Let Γ be an ω -limit cycle. If $\Gamma = L_\omega(x)$, $x \notin \Gamma$ then x has a neighborhood V such that $\Gamma = L_\omega(y)$ for all $y \in V$. In other words the set,*

$$A = \{y \mid \Gamma = L_\omega(y)\} - \Gamma$$

is open.

PROOF. Suppose Γ is an ω -limit cycle and let $\phi_t(x)$ approach Γ as $t \rightarrow \infty$. Let S be a local section at $z \in \Gamma$. Then there exists an interval $T \subset S$ which is disjoint from Γ and bounded by ϕ_{t_0}, ϕ_{t_1} with $t_0 < t_1$ and not meeting the solution of x for $t_0 < t < t_1$. The region A bounded by Γ, T , and the curve,

$$\{\phi_t(x) \mid t_0 < t < t_1\}$$

is positively invariant as is the set $B = A - \Gamma$. It follows that $\phi_t(x) \rightarrow \Gamma$ for all $y \in A$. For $t > 0$ and large enough we have that $\phi_t(x)$ is in the interior of the set A . Thus $\phi_t(y) \in A$ for y sufficiently close to x . \square

THEOREM 25. *A nonempty compact set K that is positively invariant or negatively invariant contains either a limit cycle or an equilibrium.*

PROOF. Let K be positively invariant. If $x \in K$, then $L_\omega(x)$ is a nonempty subset of K . By the Poincaré-Bendixson theorem the set K must be a closed orbit if it contains no equilibrium point. If the invariant set is an equilibrium, then the last result follows. \square

PROPOSITION 26. *Let Γ be a closed orbit and suppose that the domain W of the dynamical system includes the whole open region U enclosed by Γ . Then U contains either an equilibrium or a limit cycle.*

PROOF. Let D be the compact set $U \cup \Gamma$ where D is invariant since no solution from U can cross Γ and hence they can never lie on the same solution. If U contains no limit cycle and no equilibrium, then, for any $x \in U$,

$$L_\omega(x) = L_\alpha(x) = \Gamma$$

by the Poincaré-Bendixson Theorem. If S is a local section at a point $z \in \Gamma$, there must exist sequences $t_n \rightarrow \infty$, $s_n \rightarrow -\infty$ such that,

$$\phi_{t_n}(x) \in S, \quad \phi_{t_n}(x) \rightarrow z,$$

and

$$\phi_{s_n}(x) \in S, \quad \phi_{s_n}(x) \rightarrow z,$$

which contradicts Proposition 20. \square

THEOREM 27. *Let Γ be a closed orbit enclosing an open set U contained in the domain W of the dynamical system. Then U contains an equilibrium.*

PROOF. The proof shall be given by contradiction.

Suppose U contains no equilibrium and let x be a point in U . If $x_n \rightarrow x$ in U and each x_n lies on a closed orbit, then x must lie on a closed orbit. If not, then the solution of x would spiral toward a limit cycle, and by Proposition 25 so would the solution of x_n .

Let $A \geq 0$ be the greatest lower bound of the areas of the regions enclosed by closed orbits in U . Let $\{\Gamma_n\}$ be a sequence of closed orbits enclosing regions of areas A_n such that $\lim_{n \rightarrow \infty} A_n = A$ and let $x_n \in \Gamma_n$.

Since $\Gamma \cup U$ is compact we can assume that $x_n \rightarrow x \in U$. If U contains no equilibrium then x lies on a closed orbit β of area $A(\beta)$. As $n \rightarrow \infty$, Γ_n gets arbitrarily close to β and hence the area $A_n - A(\beta)$, of the region between Γ_n and β goes to zero and consequently $A(\beta) = A$.

Hence if U contains no equilibrium, it contains a closed orbit β enclosing a region of minimal area. Thus, the region enclosed by β contains neither a closed orbit nor an equilibrium, which contradicts Proposition 2. \square

Since planar systems allow for limit cycle solutions as a possibility, and because the stability of a solution can depend on the parameters of the system, we study bifurcation diagrams which help us to visualize the possible behaviors that occur as certain parameters are varied. In the next section we consider one special type of bifurcation point which occurs naturally after concluding the discussion on limit cycles.

2.4. The Hopf-Bifurcation

Many physical systems depend on constants, or parameters, that can have a large impact on the fate of the system. We are interested in situations where, as a parameter

is varied, the system experiences a shift in its qualitative behavior (usually in terms of its stability).

We modify (2.1.1) to include the parameter μ and obtain,

$$(2.4.1) \quad x' = f(x, \mu)$$

where μ is regarded as the bifurcation parameter. When a system bifurcates we are referring to a change in the stability of the system as the bifurcation parameter is changed. The set of (x, μ) satisfying $f(x, \mu) = 0$ is called the bifurcation diagram or solution set of f . It is necessary to note that such solution sets often do not represent functions since the stability type depends on two variables, the state variable x , and the bifurcation parameter μ .

A Hopf-Bifurcation occurs when an equilibrium point of a dynamical system loses stability as a pair of complex conjugate eigenvalues of the linearization around the equilibrium point cross the imaginary axis of the complex plane. This phenomenon often creates a branch of limit cycles from the equilibrium point.

The following theorem comes from [9, pg.342], and establishes a result for the planar Hopf-Bifurcation.

THEOREM 28 (The Hopf-Bifurcation Theorem for the case $n = 2$). *Consider the system of two differential equations which contains a parameter μ ,*

$$(2.4.2) \quad \begin{aligned} \frac{dx_1}{dt} &= f_1(x_1, x_2, \mu) \\ \frac{dx_2}{dt} &= f_2(x_1, x_2, \mu) \end{aligned}$$

where f_1 and f_2 are continuous and have partial derivatives. Suppose that for each value of μ the equations admit a steady state whose value may depend on μ , that is

$(\bar{x}(\mu), \bar{y}(\mu))$, and consider the Jacobian matrix evaluated at the parameter-dependent steady state,

$$J(\mu) = \begin{pmatrix} \frac{\partial f_1}{\partial x_1} & \frac{\partial f_1}{\partial x_2} \\ \frac{\partial f_2}{\partial x_1} & \frac{\partial f_2}{\partial x_2} \end{pmatrix}_{(\bar{x}, \bar{y})}$$

Suppose eigenvalues of this matrix are $\lambda(\mu) = a(\mu) \pm b(\mu)i$. Also suppose that there is a value μ^* , called the bifurcation value, such that $a(\mu^*) = 0$, $b(\mu^*) \neq 0$, and as μ is varied through μ^* , the real parts of the eigenvalues change signs ($\frac{da}{d\mu} \neq 0$ at $\mu = \mu^*$). Then the following three are possible,

(i) At the value $\mu = \mu^*$ a center is created at the steady state, and thus infinitely many neutrally stable concentric closed orbits surround the point (\bar{x}, \bar{y}) .

(ii) There is a range of μ values such that $\mu^* < \mu < c$ for which a single closed orbit (a limit cycle) surrounds (\bar{x}, \bar{y}) . As μ is varied, the diameter of the limit cycle changes in proportion to $|\mu - \mu^*|^{1/2}$. There are no other closed orbits near (\bar{x}, \bar{y}) . Since the limit cycle exists for μ values above μ^* , this phenomenon is known as a supercritical bifurcation.

(iii) There is a range of values such that $d < \mu < \mu^*$ for which a conclusion similar to case (ii) holds, and it is called a subcritical bifurcation.

Theorem 28 has also been generalized in [9, pg.344] for a system of n -equations. To do this consider the following system,

$$(2.4.3) \quad \begin{aligned} \frac{dx_1}{dt} &= f_1(x_1, x_2, \dots, x_n, \mu) \\ \frac{dx_2}{dt} &= f_2(x_1, x_2, \dots, x_n, \mu) \\ &\vdots \quad \quad \quad \vdots \\ \frac{dx_n}{dt} &= f_n(x_1, x_2, \dots, x_n, \mu). \end{aligned}$$

THEOREM 29 (The Hopf-Bifurcation Theorem for the case $n > 2$). *Consider the system of n variables in (2.4.3), with the appropriate smoothness assumptions on f_i , which are functions of the variables and the parameter μ . If \bar{x} is an equilibrium point of this system and linearization about this equilibrium point yields n eigenvalues,*

$$\lambda_1, \lambda_2, \dots, \lambda_{n-2}, a + bi, a - bi$$

where eigenvalues λ_1 through λ_{n-2} have negative real parts and exactly λ_{n-1}, λ_n are complex conjugates that cross the imaginary axis when μ varies through some critical value, then there exist limit-cycle solutions.

The following stability criterion was devised in [16, pgs.104-130] and can sometimes determine whether a limit cycle is stable or unstable.

THEOREM 30. *Suppose the system (2.4.2) for $\mu = \mu^*$ has the Jacobian matrix of the form,*

$$J(\bar{x}, \bar{y})|_{\mu=\mu^*} = \begin{pmatrix} 0 & 1 \\ -b & 0 \end{pmatrix}$$

which has eigenvalues $\lambda_1 = bi$ and $\lambda_2 = -bi$. Then for,

$$(2.4.4) \quad V''' = \frac{3\pi}{4b} (f_{xxx} + f_{xyy} + g_{xxy} + g_{yyy}) \\ + \frac{3\pi}{4b^2} [f_{xy} (f_{xx} + f_{yy}) + g_{xy} (g_{xx} + g_{yy}) + f_{xx}g_{xx} - f_{yy}g_{yy}]$$

evaluated at $(\bar{x}, \bar{y}, \mu^)$ the conclusions are as follows,*

- (i) If $V''' < 0$, then the limit cycle occurs for $\mu > \mu^*$ (supercritical) and is stable.*
- (ii) If $V''' > 0$, the limit cycle occurs for $\mu < \mu^*$ (subcritical) and is unstable.*
- (iii) If $V''' = 0$, the test is inconclusive.*

The following example illustrates the above theorems.

EXAMPLE 31. Consider the planar system,

$$(2.4.5) \quad \begin{aligned} \frac{dx_1}{dt} &= x_2 \\ \frac{dx_2}{dt} &= -a((x_1 - \hat{u})^2 - \eta^2)x_2 - x_1^3 + 3(x_1 + 1) - \mu \end{aligned}$$

where the set of parameters $\{a, \hat{u}, \eta\}$ are fixed and μ is the bifurcation parameter.

The bifurcation diagram for this system is generated below,

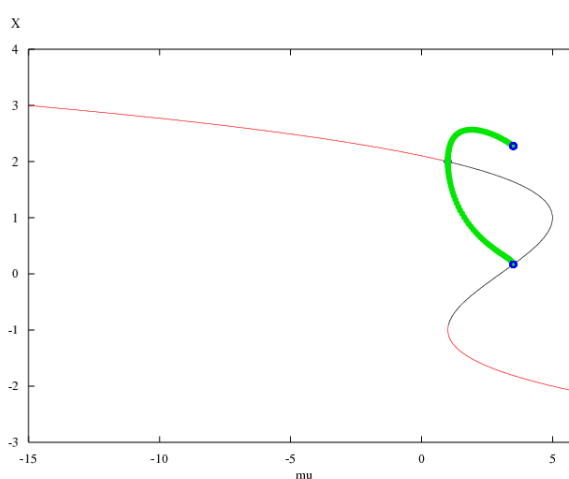


FIGURE 2.4.1. A Hopf-Bifurcation occurs at $(2,0)$ for $\mu = 1$.

Let the parameters be $a = 1$, $\hat{u} = 1.5$, and $\eta = 0.5$. The red curve represents stable equilibrium points, the black curve represents unstable equilibrium points, and the green branches represent limit cycles that occur as a result of the Hopf-Bifurcation. Notice that for μ between 1 and approximately 3.5 there exist limit cycles that surround the unstable equilibrium points.

The Jacobian of (2.4.5) is,

$$J = \begin{pmatrix} 0 & 1 \\ -2x_1x_2 + 3x_2 - 3x_1^2 + 3 & -((x_1 - 1.5)^2 - 0.25) \end{pmatrix}$$

and hence for $\mu = \mu^* = 1$ and the steady state $(2, 0)$ we obtain,

$$J((2, 0), \mu^*) = \begin{pmatrix} 0 & 1 \\ -9 & 0 \end{pmatrix}$$

which has eigenvalues $\lambda_1 = 9i$ and $\lambda_2 = -9i$. From the diagram we see that the bifurcation value $\mu^* = 1$ is supercritical. We verify this using Theorem 30 as follows. First notice that with the exclusion of the zero terms from (2.4.4) the condition for (2.4.5) simplifies to,

$$V'''(x, y) = \frac{3\pi}{4(9)}g_{xxx} + \frac{3\pi}{4(81)}g_{xx}g_{xy}$$

and when evaluated at the equilibrium point $(2, 0)$ yields,

$$V''' = -\frac{\pi}{18} < 0$$

which is a stable supercritical limit cycle as we expected.

2.5. Modeling Interacting Populations

In most real-life situations there are more than two interacting populations involved. For example there are a billions of cells interacting in the body at any given moment. Modeling this is mathematically intractable, so we often determine which populations are the most important, and only consider these populations in the model. In the preceding section we studied some planar dynamical system results, and these results can often be used as building blocks to study larger systems. In general though, the study of multipopulation models is very complicated, and planar results do not have direct analogues to higher dimensions.

Consider a system comprised of n populations, x_1, x_2, \dots, x_n , where we assume that x_1, x_2, \dots, x_n are continuously differentiable functions of t whose derivatives are functions of n population sizes at the same time. We can then write the system of n populations as,

$$\begin{aligned}
 (2.5.1) \quad \frac{dx_1}{dt} &= f_1(x_1, x_2, \dots, x_n) \\
 \frac{dx_2}{dt} &= f_2(x_1, x_2, \dots, x_n) \\
 &\vdots \quad \quad \quad \vdots \\
 \frac{dx_n}{dt} &= f_n(x_1, x_2, \dots, x_n).
 \end{aligned}$$

As in the study of single-population models [4, 5, 6, 19], the assumptions that lead to the form of (2.5.1) neglect many factors of importance in multi-population dynamics, but the model is a useful first step and may still model some real population dynamics quite well.

The system (2.5.1) is a standard way to express a system of n -autonomous differential equations, or a dynamical system. For (2.5.1) the flow would be defined as follows, $\phi : \mathbb{R} \times \mathbb{R}^n \rightarrow \mathbb{R}^n$, where we let $S = \mathbb{R}^n$, and $t \in \mathbb{R}$ as usual. This notation provides a natural extension into Chapter 3, where we study the dynamics obtained when two or three cell populations interact with each other. In Chapter 3 we consider two models, one with $n = 2$ and one with $n = 3$. Let's consider the $n = 3$ case briefly. The extension is that for $n = 3$, there are three equations which take the following form,

$$\begin{aligned}
 \frac{dx_1}{dt} &= f_1(x_1, x_2, x_3) \\
 \frac{dx_2}{dt} &= f_2(x_1, x_2, x_3) \\
 \frac{dx_3}{dt} &= f_3(x_1, x_2, x_3).
 \end{aligned}$$

The functions $f_1(x_1, x_2, x_3)$, $f_2(x_1, x_2, x_3)$, and $f_3(x_1, x_2, x_3)$ are formulated using certain hypothesis relevant to the problem. For us, the problem in Chapter 3 is biological in nature, so some appropriate assumptions have been made with respect to those

interactions. In the next section we see how the general framework considered in Section 2.2, regarding equilibria and linearization, carries over into the \mathbb{R}^n case.

2.5.1. Equilibria and Linearization in \mathbb{R}^n . According to the general framework of Section 2.2 an equilibrium in \mathbb{R}^n will be a solution $(\bar{x}_1, \bar{x}_2, \dots, \bar{x}_n)$ of (2.5.1) which is set equal to zero, i.e.,

$$(2.5.2) \quad \begin{aligned} x'_1 = \frac{dx_1}{dt} &= f_1(\bar{x}_1, \bar{x}_2, \dots, \bar{x}_n) = 0 \\ x'_2 = \frac{dx_2}{dt} &= f_2(\bar{x}_1, \bar{x}_2, \dots, \bar{x}_n) = 0 \\ &\vdots \quad \quad \quad \vdots \\ x'_n = \frac{dx_n}{dt} &= f_n(\bar{x}_1, \bar{x}_2, \dots, \bar{x}_n) = 0. \end{aligned}$$

Thus, an equilibrium is a constant solution of the system of differential equations. If $(\bar{x}_1, \bar{x}_2, \dots, \bar{x}_n)$ is an equilibrium, we can make a change of variables,

$$\begin{aligned} u_1 &= x_1 - \bar{x}_1 \\ &\vdots \quad \quad \quad \vdots \\ u_n &= x_n - \bar{x}_n \end{aligned}$$

which yields the system,

$$(2.5.3) \quad \begin{aligned} u'_1 &= f_1(\bar{x}_1 + u_1, \bar{x}_2 + u_2, \dots, \bar{x}_n + u_n) \\ &\vdots \quad \quad \quad \vdots \\ u'_n &= f_n(\bar{x}_1 + u_1, \bar{x}_2 + u_2, \dots, \bar{x}_n + u_n). \end{aligned}$$

Using the Taylor expansion for functions of n variables we may write,

which is called the Jacobian matrix at $(\bar{x}_1, \dots, \bar{x}_n)$ and was previously denoted by $D(f(\bar{x}))$.

The system (2.5.1) can be written in the vector form,

$$(2.5.5) \quad \mathbf{x}' = F(\mathbf{x}),$$

and an equilibrium is a vector \mathbf{x} satisfying $F(\bar{\mathbf{x}}) = 0$. We write the linearization of (2.5.5) as,

$$\mathbf{u}' = A\mathbf{u}$$

where $A = D(f(\bar{\mathbf{x}}))$.

The general theorem described in Subsection 2.2.1 suggests that an equilibrium of the system (2.5.2) is asymptotically stable if all solutions of the linearization at this equilibrium tend to zero (as a result of the eigenvalues all having negative real part) as $t \rightarrow \infty$, while an equilibrium \bar{x} is unstable if the linearization has any solution that grows unbounded exponentially. It is also true that all solutions of the linearization tend to zero if all roots of the characteristic equation,

$$(2.5.6) \quad \det(A - \lambda I) = 0$$

have negative real part and that the solutions of the linearization grow exponentially unbounded if (2.5.6) has any roots with positive real part. The roots of (2.5.6) are the eigenvalues of the matrix A . The characteristic equation has the property that its roots are the value of λ such that the linearization has a solution $e^{\lambda t} \mathbf{c}$ for some constant column vector \mathbf{c} . Thus the stability of an equilibrium \bar{x} can be determined from the eigenvalues of A as was seen in Subsection 2.2.1.

The characteristic equation for the n -dimensional system is a polynomial equation of degree n for which it may be difficult or impossible to find all roots explicitly. Nevertheless there does exist a general criteria for determining all roots of a polynomial equation having negative real part, and it is known as the Ruth-Hurwitz criteria [6, pg.216]. This gives the condition on a polynomial equation,

$$\lambda^n + a_1\lambda^{n-1} + \cdots + a_{n-1}\lambda + a_n = 0$$

under which all roots have negative real part.

For $n = 2$, the Ruth-Hurwitz criteria conditions are $a_1 > 0$ and $a_2 > 0$ (equivalent to the conditions that the trace of the matrix A is negative, and the determinant of the matrix A is positive). For $n = 3$ the Ruth-Hurwitz criteria conditions are $a_1 > 0$, $a_3 > 0$, and $a_1a_2 > a_3$. For a polynomial of degree n there are n conditions. As a result of this, the Ruth-Hurwitz criteria may be useful on occasion, but it can become cumbersome to apply to problems of higher dimensions.

For planar autonomous systems, the Poincaré-Bendixson theorem makes it possible to analyze the qualitative behavior of a system under very general conditions. Essentially we know that a bounded orbit must approach either an equilibrium or a limit cycle. For autonomous systems consisting of more than two differential equations a much larger range of behavior is possible.

Biological evidence suggests that more complicated interacting population systems have a tendency to be more stable than simple systems. For example, in a predator-prey model a predator population can switch between different prey populations, since its food supply may be less sensitive to disturbances than if it were dependent on a single food supply [9]. On the other hand the removal of one population can lead to the collapse of a population in the system. The relationship between stability and population systems, a question raised by [17], is not well understood. In the following Chapter one of the important things we will study is how adding an additional population into a model can change the qualitative behavior of the solutions.

This implies that the predictive power of a model is highly contingent on making sure as many of the essential variables have been considered in the model as possible.

CHAPTER 3

A Mathematical Modeling of Tumor Growth

A tumor forms when cancerous cells in the body are allowed to grow without bound due to the immune system perceiving them as “self” cells [1, 14]. One of the ways tumors develop is when the mechanisms that control cell growth and differentiation malfunction. Many of the treatments used to combat cancer yield only temporary results due to the ability of cancer cells to go undetected by the immune system and replicate themselves at a high rate. In order for treatments to be successful they must either completely eradicate all cancer cells from the body, or remove enough of them to allow the immune system to combat the remaining tumor cells. However, since the strength of the immune system varies from individual to individual the outcome of the treatments vary greatly [20]. In the succeeding sections we study a model which accounts for the effect of the immune system on the population of tumor cells.

3.1. Model 1 - Analysis of the Effector/Tumor Cell Interaction

3.1.1. Required Biology. When cancerous tumor cells are present in a person, one of the first lines of defense is offered by the immune system. Within the body there are always present immune system cells, or effector cells, such as cytotoxic T-lymphocytes (CTL) and natural killer cells (NK) which work to kill tumor cells. For most people, spontaneously arising tumors grow out of control, and the immune system alone is incapable of fighting the tumor in a way that allows the person to survive. As a result of this, many different therapies have been developed, and one such therapy is considered in Section 3.2 when we study Model 2. For now the model we consider will have no therapies, and instead will focus on how the immune system alone is capable of handling the tumor. The term *immunogenic* refers to tumor cells

which are subject to be attacked by CTL or NK cells. In contrast, some tumor cells are able to sneak past the CTL and NK cells because the immune system sees them as a part of the “self”. In Model 1 we find several different possibilities as a result of our stability analysis, and an interesting exclusion of closed orbits as a result of the Dulac-Bendixson criterion. These results will be followed by a bifurcation analysis.

3.1.2. Development and Description of Model 1. Let $E(t)$ be the population of CTL and NK cells, and $T(t)$ be the population of tumor cells. Then the model developed in [14] is,

$$(3.1.1) \quad \begin{aligned} \frac{dE}{dt} &= s + \frac{p_1 ET}{g_1 + T} - mET - dE \\ \frac{dT}{dt} &= r_2 T(1 - bT) - nET \end{aligned}$$

with initial conditions $E(0) = E_0$ and $T(0) = T_0$.

In the first equation of (3.1.1) the quantity s represents a constant production of effector cells, $\frac{p_1 ET}{g_1 + T}$ the assumed Michaelis-Menten kinetics (see Appendix, 5.2) between E and T with rate p_1 . mET is the removal of effector cells from the system as they expire fighting off the tumor cells, and dE represents the natural death rate of the effector cells. For the Michaelis-Menten term, the quantity p_1 represents the limiting or saturation population as $t \rightarrow \infty$, and when $t = g_1$ exactly half of the saturation has been achieved.

In the second equation of (3.1.1) the quantity $r_2 T(1 - bT)$ represents the logistic growth of the tumor cells as was determined experimentally in [14] and nET is the removal of tumor cells from the system as they are killed by the effector cells.

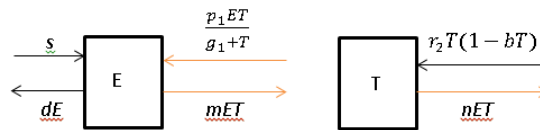


FIGURE 3.1.1. A diagram of system (3.1.1).

3.1.3. Parameter Estimation. Using data acquired from a variety of sources [14] was able to estimate the parameters in (3.1.1) and the results are recorded below in Table 1.

Eq. (1)	$s = 1.3 \times 10^4 \frac{\text{cells}}{\text{day}}$	$p_1 = 0.1245 \text{ day}^{-1}$	$g_1 = 2.019 \times 10^7 \text{ cells}$
	$m = 3.422 \times 10^{-10} \frac{1}{\text{day cells}}$	$d = 0.0412 \text{ day}^{-1}$	
Eq. (2)	$r_2 = 0.18 \text{ day}^{-1}$	$b = 2.0 \times 10^9 \text{ cells}^{-1}$	$n = 1.101 \times 10^{-7} \frac{1}{\text{day cells}}$

Table 1: Parameter Values

3.1.4. Nondimensionalization of the System. From Table 1 it is apparent that the system given in (3.1.1) has parameter values with vastly different scales. As a result of this we non-dimensionalize (see Appendix 5.1) the system so that the numerical techniques used by the computer algebra systems will be more stable.

$$x = \frac{E}{E_0}, \quad y = \frac{T}{T_0}, \quad \tau = nT_0t,$$

$$\sigma = \frac{s}{nE_0T_0}, \quad \rho = \frac{p_1}{nT_0}, \quad \eta = \frac{g_1}{T_0},$$

$$\alpha = \frac{r_2}{nT_0}, \quad \delta = \frac{d}{nT_0}, \quad \mu = \frac{m}{n} \quad \beta = bT_0.$$

The above scaling yields the following scaled system after substitution,

$$(3.1.2) \quad \begin{aligned} \frac{dx}{d\tau} &= \sigma + \frac{\rho xy}{\eta + y} - \mu xy - \delta x \\ \frac{dy}{d\tau} &= \alpha y(1 - \beta y) - xy. \end{aligned}$$

We then obtain the following set of non-dimensional parameters,

Eq. (1)	$\sigma = 0.1181$	$\rho = 1.131$	$\eta = 20.19$	$\mu = 0.00311$	$\delta = 0.3743$
Eq. (2)	$\alpha = 1.636$	$\beta = 2.0 \times 10^{-3}$			

Table 2: Parameter Values

3.1.5. Stability Analysis. To determine the fixed points of (3.1.2) we employ nullcline analysis. There is only one nullcline for the equation $\frac{dx}{d\tau} = 0$ and it is,

$$f(y) \equiv x = \frac{\sigma}{\delta + \mu y - \frac{\rho y}{\eta + y}}.$$

There are two nullclines for the equation $\frac{dy}{d\tau} = 0$ and they are,

$$y = 0 \quad \text{and} \quad g(y) \equiv x = \alpha(1 - \beta y).$$

The intersection of $y = 0$ and $f(y)$ yields $e_1 = \left(\frac{\sigma}{\delta}, 0\right)$ as an equilibrium point of the system. The intersection of $f(y)$ and $g(y)$,

$$\alpha(1 - \beta y) = \frac{\sigma}{\delta + \mu y - \frac{\rho y}{\eta + y}}$$

yields, after some algebra, the third degree polynomial,

$$a_3 y^3 + a_2 y^2 + a_1 y + a_0 = 0$$

where,

$$\begin{aligned} a_0 &= \eta \left(\frac{\sigma}{\alpha} - \delta \right), & a_1 &= \frac{\sigma}{\alpha} + \rho - \mu\eta - \delta + \delta\eta\beta \\ a_2 &= -\mu + (\mu\eta + \delta - p)\beta & \text{and} & \quad a_3 = \mu\beta \end{aligned}$$

It was shown in [14, pg.14] that there exist between 1 and 4 equilibrium points depending on the values of a_0, a_1, a_2 , and a_3 .

The Jacobian of the system is,

$$J = \begin{pmatrix} \frac{\rho y}{\eta+y} - \mu y - \delta & \frac{\rho x \eta}{(\eta+y)^2} - \mu x \\ -y & \alpha - 2\alpha\beta y - xy \end{pmatrix}$$

For $e_1 = (\frac{\sigma}{\delta}, 0)$ we have,

$$J(e_1) = \begin{pmatrix} -\delta & \frac{\rho\eta}{\delta n} - \frac{\mu\sigma}{\delta} \\ 0 & \alpha - \frac{\sigma}{\delta} \end{pmatrix}.$$

The eigenvalues are $\lambda_1 = -\delta$ and $\lambda_2 = \alpha - \frac{\sigma}{\delta}$ which yields an unstable saddle point when $\alpha > \frac{\sigma}{\delta}$, and a stable equilibrium point when $\alpha < \frac{\sigma}{\delta}$.

3.1.6. Typical Solution Curves. Using the dimensionless quantities in (3.1.2) and the parameters in Table 2, we now plot the nullclines along with some solutions of the system.

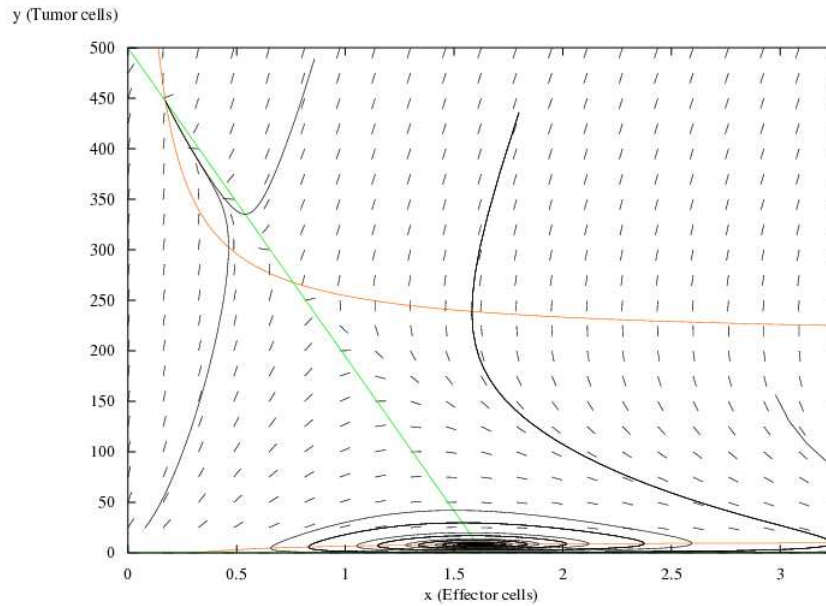


FIGURE 3.1.2. Phase portrait for (3.1.2) with parameters from Table 2.

From Figure 3.1.2 it is evident from the intersection of the nullclines that there are three equilibrium points, two stable equilibria and one saddle point.

3.1.7. Nonexistence of Limit Cycles. The system (3.1.2) contains no closed orbits, and therefore no limit cycles as a result of the Dulac-Bendixson criterion (see Appendix 5.3). Consider the function $M = \frac{1}{xy}$. Then,

$$\begin{aligned} L &\equiv \frac{\partial}{\partial x} \left(M \frac{dx}{d\tau} \right) + \frac{\partial}{\partial y} \left(M \frac{dy}{d\tau} \right) \\ &= \frac{\partial}{\partial x} \left(\frac{1}{xy} \left(\sigma + \frac{\rho xy}{\eta + y} - \mu xy - \delta x \right) \right) + \frac{\partial}{\partial y} \left(\frac{1}{xy} (\alpha y(1 - \beta y) - xy) \right) \\ &= -\frac{\sigma}{x^2 y} - \frac{\alpha \beta}{x} \\ &= -\left(\frac{\sigma}{x^2 y} + \frac{\alpha \beta}{x} \right) < 0 \end{aligned}$$

because $x, y, \alpha, \beta, \sigma > 0$. Since there exist no closed orbits in the system, we conclude that the spiraling equilibrium point found in Figure 3.1.2 must be an asymptotically stable sink.

3.1.8. Bifurcation Analysis of Model 1. We now employ a bifurcation analysis on the parameter σ which was highlighted by [14] to be a parameter of interest. Before proceeding we note that the nonexistence of limit cycles excludes Hopf-Bifurcations as a possibility from the analysis.

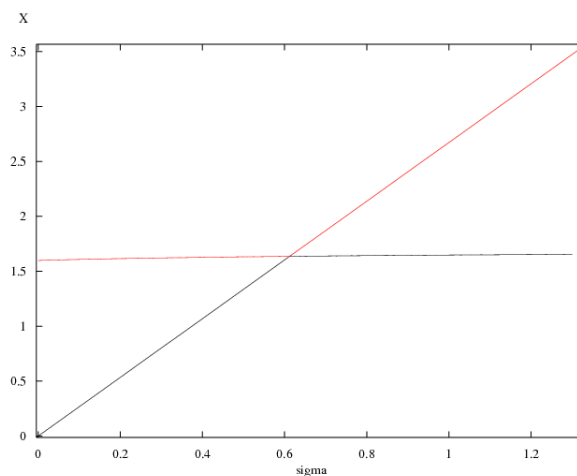


FIGURE 3.1.3. Transcritical Bifurcation for $0 \leq \sigma \leq 1.3$.

We observe a transcritical bifurcation (see Appendix, 5.4) in the system as the parameter σ is varied. The black line represents unstable equilibrium points, and the red line represents stable equilibrium points. The place where the bifurcation occurs is for $\sigma_{TB} = 0.6124$, $x = 1.636$, and $y = 9.544 \times 10^{-7}$ respectively. This tells us that for parameter values just to the left or right of σ_{TB} the system will exhibit qualitatively different behavior as the stability of the equilibrium point changes for values on either side of σ_{TB} .

3.2. Model 2 - Inclusion of IL-2

3.2.1. Additional Required Biology. Methods outside of chemo- and radiotherapies and surgeries, which often lead to a regression of cancer and not a cure, are being thoroughly investigated by oncologists. One such method is that of immunotherapy, which refers to the use of cytokines usually together with adoptive cellular immunotherapy (ACI). ACI refers to a treatment in which cultured immune cells with anti-tumor properties are applied to a tumor. Cytokines are protein hormones that bolster the bodies immunity. Interleukin-2 (IL-2) is the primary cytokine responsible for lymphocyte activation and growth. Essentially the lymphocytes can be seen as “good” cells whose numbers are bolstered by the presence of cytokines. As a result, the number of effector cells is bolstered by the presence of IL-2.

3.2.2. Development and Description of Model 2. In [13] the new dynamics are obtained by considering how the presence of IL-2 affects the model of Section 3.1. After studying [14] and other existing models, a model was generated that consists of three variables, namely, the effector cells $E(t)$, tumor cells $T(t)$, and the concentration of IL-2 $I_L(t)$. The model derived in [13] is,

$$(3.2.1) \quad \begin{aligned} \frac{dE}{dt} &= cT - \mu_2 E + \frac{p_1 E I_L}{g_1 + I_L} + s_1 \\ \frac{dT}{dt} &= r_2 T (1 - bT) - \frac{aET}{g_2 + T} \\ \frac{dI_L}{dt} &= \frac{p_2 ET}{g_3 + T} - \mu_3 I_L + s_2 \end{aligned}$$

with initial conditions $E(0) = E_0$, $T(0) = T_0$, and $I_L(0) = I_{L_0}$.

The parameter c in the first equation of (3.2.1) quantifies the antigenicity of the tumor, and provides a measure of the body's natural ability to detect and combat the tumor being studied. The higher the value of c , the larger the number of effector cells, and hence the better the body will be at fighting tumor cells. The second term represents the natural death of effector cells with an average lifespan of $\frac{1}{\mu_2}$. The third term represents the growth of effector cells due to the presence of IL-2, and the Michaelis-Menten form has been chosen with rate p_1 . The last term, s_1 is the treatment term which represents a constant external source of effector cells generated by ACI.

The second equation in (3.2.1) assumes a logistic rate of growth with carrying capacity $\frac{1}{b}$ for the tumor cells, and the second term removes tumor cells based on the Michaelis-Menten interaction with effector cells at rate a .

The final equation in (3.2.1) models the change in concentration of IL-2 cells with a death rate of μ_3 , and a treatment term s_2 which indicates the external input of IL-2 into the system. The presence of effector and tumor cells stimulates the production of IL-2 and the Michaelis-Menten form has been chosen with rate p_2 .

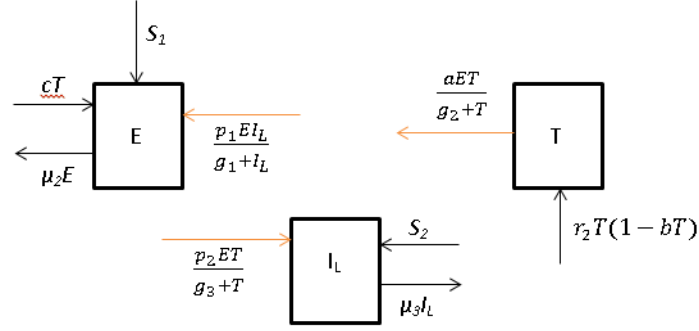


FIGURE 3.2.1. A diagram of system (3.2.1).

3.2.3. Parameter Estimation. The parameter c will be studied carefully since knowing the value of this parameter in general is not possible, as each patient will naturally have their own unique value. A patient can only hope their body has a larger value of c which represents a well recognized antigen, and a better capacity to fight the tumor as mentioned above. The authors considered many resources, including [14] and they chose the parameter values listed in Table 3 below. Note that some of the parameters are the same as in Table 1, and the units remain the same. The new parameters μ_1 and μ_2 have units of days^{-1} .

Eq. (1)	$0 \leq c \leq 0.05$	$\mu_2 = 0.03$	$p_1 = 0.1245$	$g_1 = 2 \times 10^7$
Eq. (2)	$g_2 = 1 \times 10^5$	$r_2 = 0.18$	$b = 1 \times 10^9$	$a = 1$
Eq. (3)	$\mu_3 = 10$	$p_2 = 5$	$g_3 = 1 \times 10^3$	

Table 3: Parameter Values

3.2.4. Nondimensionalization of the System. In the same way, and for the same reasons that we nondimensionalized Model 1 in Subsection 3.1.4 we nondimensionalize (3.2.1) by using the following scaling from [13],

$$x = \frac{E}{E_0}, \quad y = \frac{T}{T_0}, \quad z = \frac{I_L}{I_{L_0}}, \quad \tau = t_s t \quad \bar{c} = \frac{c T_0}{t_s E_0},$$

$$\bar{p} = \frac{p_1}{t_s}, \quad \bar{g}_1 = \frac{g_1}{I_{L_0}}, \quad \bar{\mu}_2 = \frac{\mu_2}{t_s}, \quad \bar{g}_2 = \frac{g_2}{T_0} \quad \bar{b} = b T_0,$$

$$\bar{r}_2 = \frac{r_2}{t_s}, \quad \bar{a} = \frac{aE_0}{t_s T_0}, \quad \bar{\mu}_3 = \frac{\mu_3}{t_s}, \quad \bar{p}_2 = \frac{p_2 E_0}{t_s I_{L_0}}, \quad \bar{g}_3 = \frac{g_3}{T_0},$$

$$\bar{s}_1 = \frac{s_1}{t_s E_0}, \quad \bar{s}_2 = \frac{s_2}{t_s I_{L_0}}.$$

We derive the new effector cell equation using the substitutions above, and simply write the other two. Solving for the left hand side yields,

$$\begin{cases} E = xE_0 \\ t = \frac{\tau}{t_s} \end{cases} \implies \frac{dE}{dt} = \frac{dx E_0}{d\frac{\tau}{t_s}} = t_s E_0 \frac{dx}{d\tau},$$

$$\begin{cases} T = yT_0 \\ c = \frac{\bar{c} t_s E_0}{T_0} \end{cases} \implies cT = \frac{yT_0 \bar{c} t_s E_0}{T_0} = \bar{c} t_s E_0 y,$$

$$\begin{cases} \mu_2 = \bar{\mu}_2 t_s \\ E = xE_0 \end{cases} \implies -\mu_2 E = -\bar{\mu}_2 t_s E_0 x,$$

$$\begin{cases} p_1 = \bar{p}_1 t_s \\ g_1 = \bar{g}_1 I_{L_0} \end{cases} \implies \frac{p_1 E I_L}{g_1 + I_L} = \frac{\bar{p}_1 t_s E_0 I_{L_0} x z}{\bar{g}_1 I_{L_0} + z I_{L_0}} = \frac{\bar{p}_1 t_s E_0 x z}{\bar{g}_1 + z}.$$

Notice that each expression has the factor $t_s E_0$, so dividing through by it yields,

$$\begin{aligned} \frac{dx}{d\tau} &= \bar{c} y - \bar{\mu}_2 x + \frac{\bar{p}_1 x z}{\bar{g}_1 + z} + \bar{s}_1 \\ &= c y - \mu_2 x + \frac{p_1 x z}{\bar{g}_1 + z} + s_1 \end{aligned}$$

where we obtained the second equation by dropping the bar notation on the parameters, however the parameters should be computed using the scaling defined above. We can do this exact same thing for the remaining two equations and obtain the

scaled system,

$$(3.2.2) \quad \begin{aligned} \frac{dx}{d\tau} &= cy - \mu_2 x + \frac{p_1 x z}{g_1 + z} + s_1 \\ \frac{dy}{d\tau} &= r_2 y(1 - by) - \frac{axy}{g_2 + y} \\ \frac{dz}{d\tau} &= \frac{p_2 xy}{g_3 + y} - \mu_3 z + s_2 \end{aligned}$$

with initial conditions, $x(0) = x_0$, $y(0) = y_0$, and $z(0) = z_0$.

3.2.5. Stability Analysis. The Jacobian for the system (3.2.2) is,

$$(3.2.3) \quad J = \begin{pmatrix} -\mu_2 + \frac{p_1 z}{g_1 + z} & c & \frac{p_1 x}{g_1 + z} - \frac{p_1 x z}{(g_1 + z)^2} \\ \frac{-ay}{g_2 + y} & r_2 - 2br_2 y - \frac{ax}{g_2 + y} + \frac{axy}{(g_2 + y)^2} & 0 \\ \frac{p_2 y}{g_3 + y} & \frac{p_2 x}{g_3 + y} - \frac{p_2 xy}{(g_3 + y)^2} & -\mu_3 \end{pmatrix}$$

Consider the trivial equilibrium point $e_0 = (0, 0, 0)$. When we evaluate (3.2.3) at the trivial equilibrium point we obtain the matrix,

$$J(e_0) = \begin{pmatrix} -\mu_2 & c & 0 \\ 0 & r_2 & 0 \\ 0 & 0 & -\mu_3 \end{pmatrix}$$

This equilibrium point has a combination of positive and negative eigenvalues, and hence is a locally unstable saddle point. Analytic computation of the other equilibrium points is very difficult primarily due to the presence of the Michaelis-Menten terms.

3.2.6. Two Different Scalings, One Result. Note that for now and until Section 3.2.9 we will consider (3.2.2) with $s_1 = s_2 = 0$. To confirm the qualitative behavior of the system we will use two different scalings and show that they both lead to identical output as expected. First we utilize the scaling suggested in [14] which

is $T_0 = E_0 = I_{L_0} = 1/b$, and $t_s = r_2$. This leads to the parameters shown below in Table 4 with a carrying capacity of 1.

Eq. (1)	$0 \leq c \leq 0.27777$	$\mu_2 = 0.16666$	$p_1 = 0.69166$	$g_1 = 0.02$
Eq. (2)	$g_2 = 0.0001$	$r_2 = 1$	$b = 1$	$a = 5.55555$
Eq. (3)	$\mu_3 = 55.55555$	$p_2 = 27.77777$	$g_3 = 1 \times 10^{-6}$	

Table 4: Parameter Values

Notice the scaling suggested in [13] has a time scale which is reduced to 18% of the original. We now observe the behavior of a particular situation with the parameters in Table 4, $c = 0.083333$, and initial conditions $E_0 = T_0 = I_{L_0} = 1 \times 10^{-9}$ with the results displayed in Figure 3.2.2.

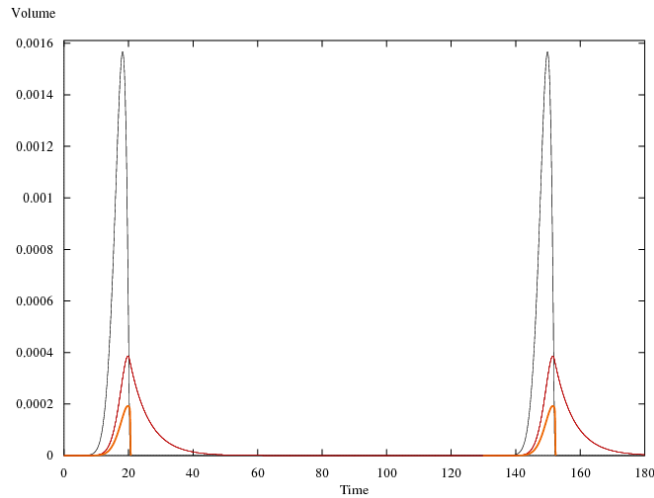


FIGURE 3.2.2. Plot using parameters in Table 4.

Next we utilize a scaling with a carrying capacity of 1×10^5 which means that $T_0 = E_0 = I_{L_0} = 1/b = 1 \times 10^5$ and we do not scale the time, i.e. $t_s = 1$. This leads to the parameters shown below in Table 5.

Eq. (1)	$0 \leq c \leq 0.05$	$\mu_2 = 0.03$	$p_1 = 0.1245$	$g_1 = 2000$
Eq. (2)	$g_2 = 10$	$r_2 = 0.18$	$b = 1 \times 10^{-5}$	$a = 1$
Eq. (3)	$\mu_3 = 10$	$p_2 = 5$	$g_3 = 0.1$	

Table 5: Parameter Values

We now observe the behavior of a particular situation with the parameters in Table 5, $c = 0.015$, and initial conditions $E_0 = T_0 = I_{L_0} = 1 \times 10^{-5}$ with the results displayed in Figure 3.2.3.

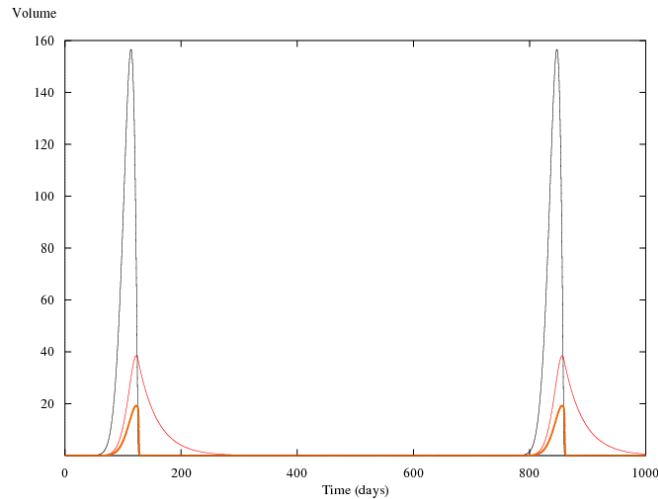


FIGURE 3.2.3. Plot using parameters in Table 5.

Comparing Figure 3.2.3 with Figure 3.2.2 we can immediately see that the behavior is identical, the only change being in the scales. Figure 3.2.3 has preserved the scale of the original problem, which was in days, whereas Figure 3.2.2 has a new scale where every time unit is approximately 4 days. Furthermore, the volume scale has changed as well, and to equal the original scale would require a multiplication of 1×10^5 which is the difference in the scaling of the two problems considered above.

3.2.7. Effects of the Antigenicity, c . Let's focus exclusively on the scaling used in Table 5, as this choice preserves the day time scale, and consider how varying the parameter c changes the solution curves. First recall that we biologically expect an increase in antigenicity to lead to a reduction in the mass of the tumor. This corresponds to an increase in the number of effector cells, which leads to a reduction in the number of tumor cells. Several solution curves have been generated on the next page, each with a different value of c . For the following graphs the red curve indicates the effector cell population, the black curve represents the tumor cell population, and the orange curve represents the IL-2 cell population.

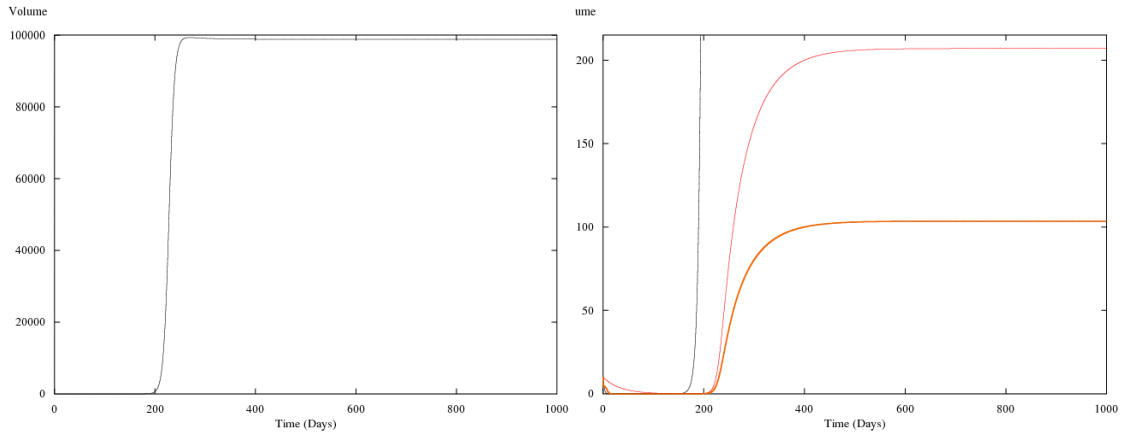


FIGURE 3.2.4. $c = 5 \times 10^{-5}$.

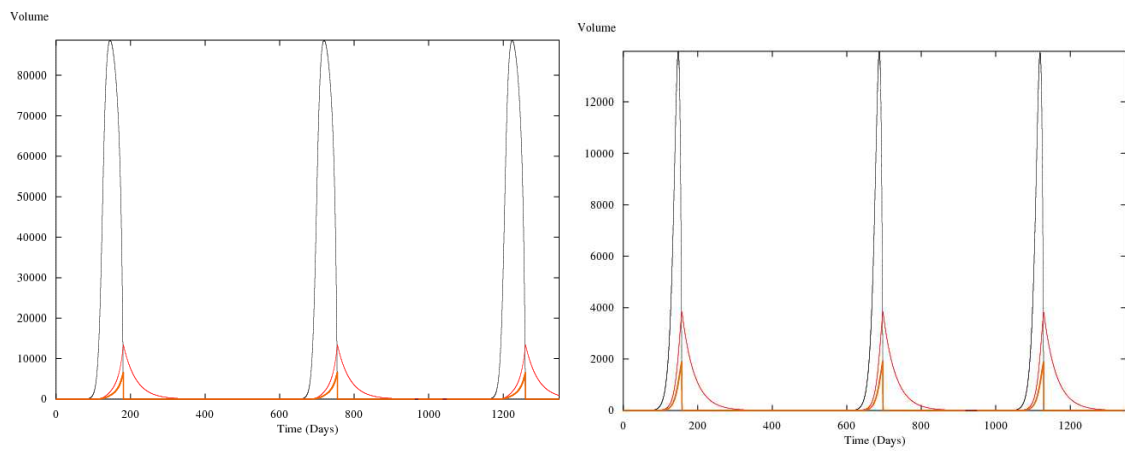


FIGURE 3.2.5. Left: $c = 0.001$. Right: $c = 0.01$.

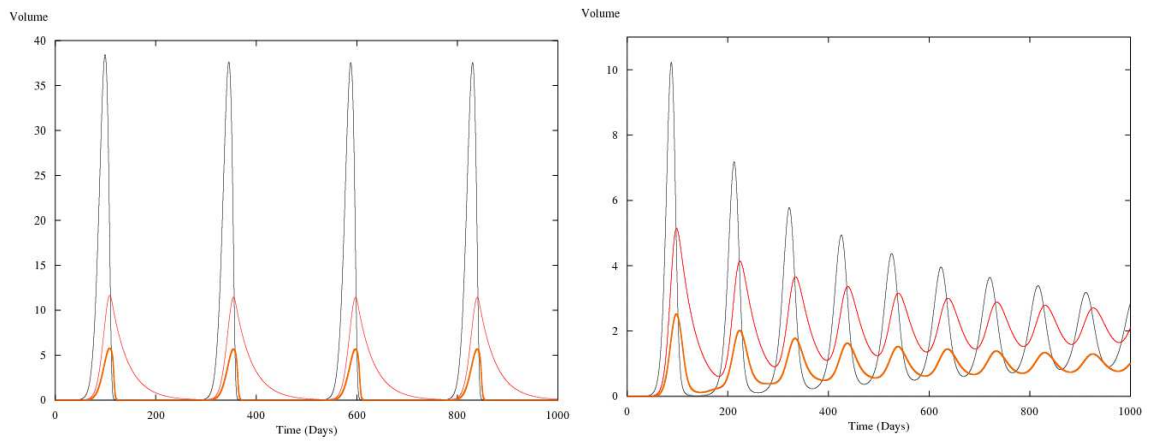


FIGURE 3.2.6. Left: $c = 0.02$. Right: $c = 0.035$.

Some very interesting results can now be mentioned. First, in Figure 3.2.4 for $c = 5 \times 10^{-5}$ we notice that the population of the tumor cell has a very sharp increase and approaches the carrying capacity of the scaled model ($\frac{1}{b} = 1 \times 10^5$) from the logistic growth assumption. The effector and IL-2 cells also approach their respective “carrying capacities” which is approximately three orders of magnitude smaller. Observe that there is an initial reduction in the number of tumor cells, however after a period of approximately 200 days there is a drastic increase in the tumor population which tends to the carrying capacity. This represents the inability to fight the small number of tumor cells due to a very small antigenicity.

The three Figures (3.2.5)-(3.2.6)(Left) all represent the same behavior which begins when $c = c_0 = 0.8552 \times 10^{-5}$ and ends when $c = c_1 = 0.03247$. We notice that the solutions are all periodic with two primary differences. The first noticeable difference is that the value of the amplitude depends heavily on the value of c , as is to be expected. For smaller values of c such as in Figure 3.2.5(Left) we notice that the amplitude of the tumor cells reaches approximately 90% of the carrying capacity, whereas for Figure 3.2.6(Left) the amplitude of the tumor cells reaches approximately 0.04% of the carrying capacity. The second noticeable difference is that as c increases the period of the solutions decrease, leading to solutions which are more oscillatory, but reach much lower tumor population levels.

In Figure 3.2.6(Right) we have an interesting situation where the amplitude of the solution curves decrease with each successive “period”. Eventually the solution will reach a stable equilibrium point whereby the tumor cell population will have a constant very small mass in comparison to the other two possibilities described above.

3.2.8. Bifurcation Analysis. The results found from the above section naturally lead to a bifurcation analysis on the antigenicity parameter c since it plays a very obvious role in determining the outcome of the solutions. From XPPAut we obtain the following bifurcation diagram.

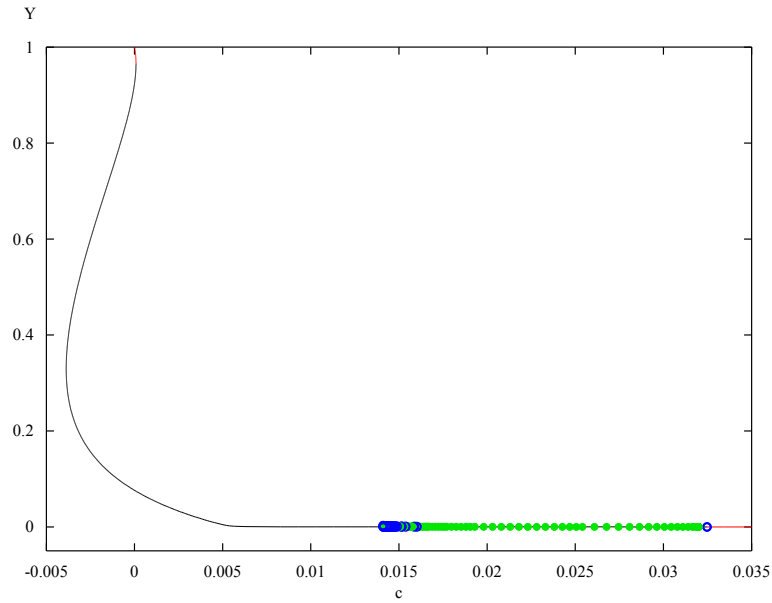


FIGURE 3.2.7. Bifurcation diagram with carrying capacity of tumor scaled to 1, and the time not scaled.

Changing the numerics on the axes allows us to see some interesting behavior.

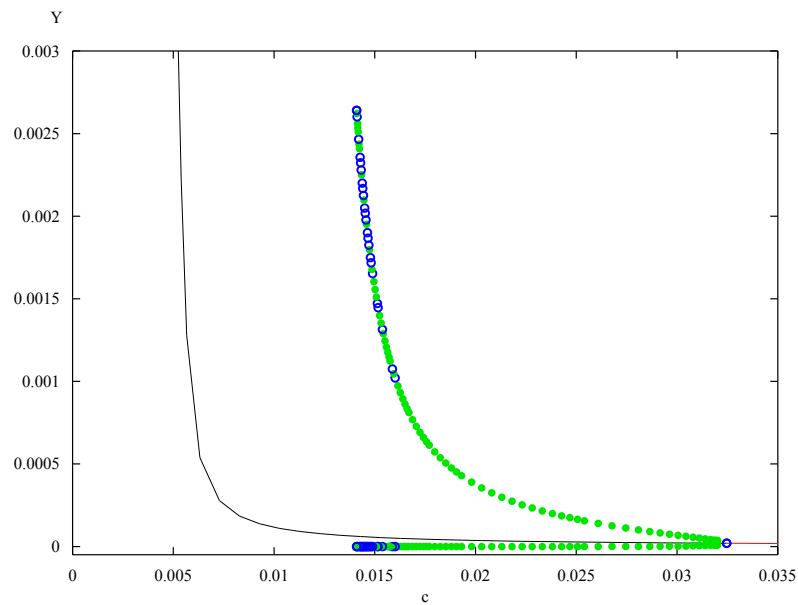


FIGURE 3.2.8. Scaled to see the Hopf-Bifurcation.

We observe a Hopf-Bifurcation occurring at $c_{HB} = 0.03247$. The Hopf-Bifurcation branch is represented by the green and blue curve where we see the branch surround an unstable equilibrium point and hence c_{HB} is a supercritical bifurcation point. This

behavior has also been captured numerically, as we can plot solutions just to the left of c_{HB} and observe limit cycles, and plot values just to the right of c_{HB} and observe periodic solutions with decreasing amplitudes that tend toward a small mass tumor.

A consequence of the bifurcation diagram is a plot of how the period changes as the parameter c is changed, and such a plot has been generated below.

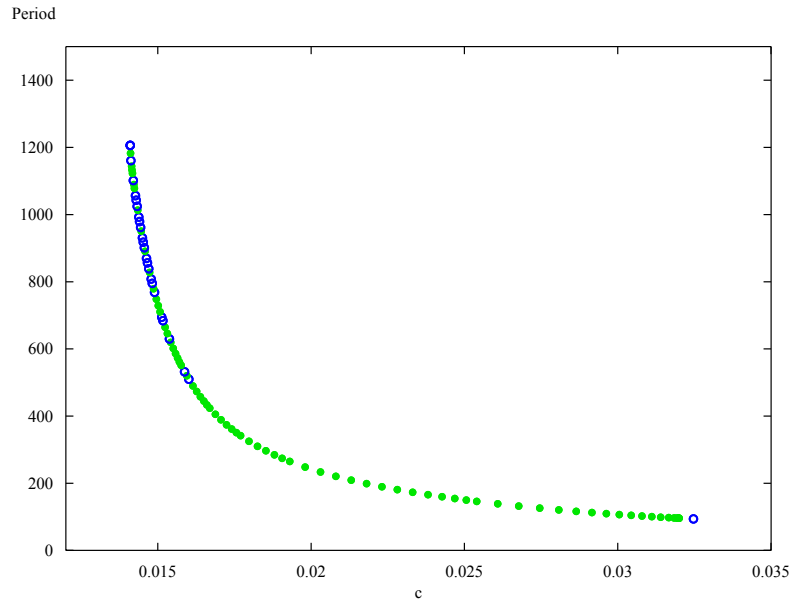


FIGURE 3.2.9. c vs period.

It is evident that for smaller values of c the period increases, which means that not only are the tumors getting larger in size, but they stay larger for longer periods of time. This makes sense since as c approaches c_0 we expect the tumor to get closer and closer to the carrying capacity.

3.2.9. Treatment. According to [7, 20] real life treatment is not continuous as was assumed in [13], but instead occurs as large dosages for a certain cycle length. Suppose the value s_2 instead of being constant, is a function of time and the effector cell population. The study in [20] provides a methodology that was used to treat patients with two different types of cancer using immunotherapy. Treatment was administered intravenously over 15 minutes every 8 hours or until grade 3 or 4 toxicity was reached. The toxicity grade provides a measure for how negative the impact of treatment is on the patient. Each treatment course consisted of two cycles containing a maximum of 15 doses of IL-2 per cycle. Approximately 10 days after completing the first cycle of treatment, patients began to receive the second cycle [20]. This implies that the treatment was continuous only over the course of 15 minutes, which is a very short time scale for our model where the time is in days. First we attempt to model the treatment described above in [20]. The MATLAB output is provided in Figure 3.2.10 below.

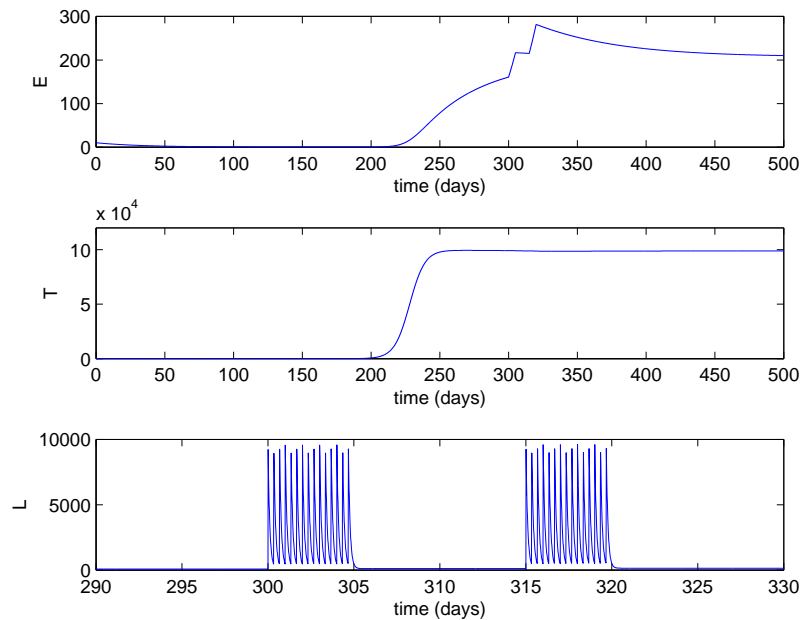


FIGURE 3.2.10. Plot of impact of treatment from [20].

Treatments used to generate the above figure were given for 15 minutes, 8 times per day, 10 days apart, and for 2 cycles. According to the model the described treatment should have no impact on the tumor cell population, however this is not true since in real life according to [20] 19% of the patients in the study experienced complete or partial regression of their respective cancers. The failure of the model to capture this behavior could be due to a variety of reasons, however it was observed that for no value of c did the treatment have any considerable impact on the tumor cell population for any reasonable value of s_2 . It should be noted that without treatment and from Figure 3.2.4 it is seen that the effector cell population levels off around 200, but with the addition of the treatment it is able to briefly approach 300. This slight increase is not enough to impact the tumor cell population. A larger dose could be administered to increase the effector cell population even more, however this larger dose may not be physically possible in reality due to toxicity, and needs to be investigated further.

In [7] the situation was modeled by using an on/off switch according to an immune threshold flag which simulated the impact of toxicity on the system as a result of the IL-2 therapy. By considering similar conditions we are able to model a reduction in the tumor cell population, which is evident in Figure 3.2.11 below.

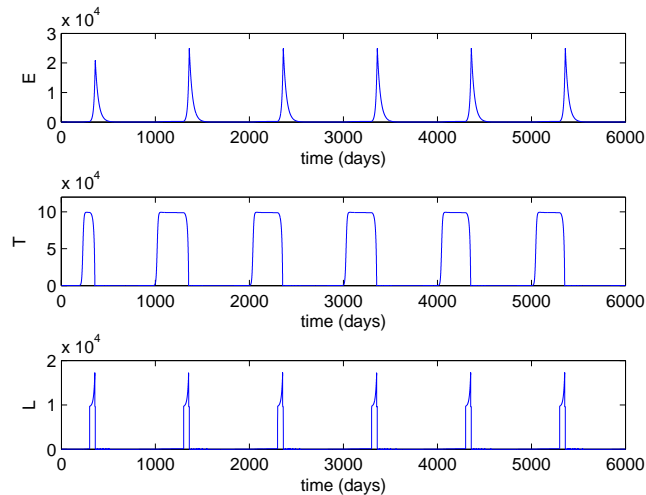


FIGURE 3.2.11. Plot of a periodic fixed-duration continuous treatment.

The treatment was initially given on day 300, lasted for 60 days, and spaced 1000 days apart. The treatment is able to regress the tumor, however only for a certain period of time before it comes back. By varying the amount of treatment s_2 , the duration of each treatment, the number of treatments, the immune response a , and the antigenicity c we are able to develop different treatment possibilities. A question to consider is would a person survive the treatment regimen used to generate Figure 3.2.11, since it varies so drastically from the study done in [20]. The number of effector cells becomes much larger due to the second treatment as a result of the continuous input of IL-2, which is the reason for the reduction in tumor mass. By considering different parameter combinations, one may be able to devise an optimal drug regimen for a certain person, however doing this would be difficult because each persons parameter values differ, and so it would have to be done on a case by case basis. In reality, these complications could be indicative of the model's limitations when treatment is included, and a more refined or advanced model may be needed.

CHAPTER 4

Concluding Remarks

In Model 2 of Chapter 3 we studied the effects of IL-2 on tumor-immune dynamics, and determined that the antigenicity c plays an important role in the long-term behavior of the system. We found that for $0 < c_0 \leq 0.8552 \times 10^{-5}$ the tumor population approaches its carrying capacity, for $0.8552 \times 10^{-5} < c_1 \leq 0.03247$ the tumor population tends to stable limit cycles of varying amplitudes and periods, and that for $c_2 > c_1$ the tumor population approaches a small constant size. All three of these possibilities have been documented in case studies [13] which provides evidence to support the different behaviors predicted by the model.

While studying Model 2 we employed two computer algebra systems to solve the problem which were XPPAut and MATLAB. While using this software it was evident that achieving accurate results not only depended on setting the appropriate absolute and relative tolerances, but was also parameter dependent, in particular on the antigenicity c . This means that the system might converge to a solution for one value of c , but fail to provide a solution for a different value of c . It is observed numerically that the system (3.2.1) is a stiff system, and it turned out that for certain values of c the traditional Runge-Kutta 4 would fail to converge. By stiff we mean that the convergence of solutions using computer algebra systems was parameter dependent. Thus we had to utilize stiff solvers such as VODE, which use variable time steps to provide a solution. It was also found that in situations where two different numerical methods were applied to the same problem with oscillatory solutions they would often differ in phase. It is not possible to know which solution is more accurate since the exact solution is unknown.

There is still much to be done in the field of tumor modeling, especially when it comes to analyzing how to best implement treatments into the model. The paper [2] continues the story by adding a fourth variable into the system we studied in Section 3.2. The system is modified to account for more possibilities that can occur when a tumor is forming in the body such as the effects of the immuno-suppressive cytokine $TGF - \beta$ which actually works to reduce the number of effector cells in the system. They then extend the model to include siRNA treatment which work to reduce the number of $TGF - \beta$ cells present, and thus again boost the effects of the immune system. It is this seemingly infinite game of tug of war that beautifully illustrates the arising complications of higher dimensional dynamical systems. Furthermore, for higher dimensional systems most of the elegant results discovered for two-dimensions are lost. While many higher dimensional systems have geometrically equivalent lower dimensional counterparts, however this is not usually the case for systems of the type studied in this paper. This inevitably leads to the use of computer algebra systems to solve higher dimensional problems, but as we have seen these can still have their limitations.

An interesting future study would be the inclusion of chemotherapy to the model developed in Section 3.2 or to the more refined model of [2]. Perhaps a mixture of less toxic treatments would lead to models which predict regression or termination of the tumor cell population. The answers to such questions may not only lead to mathematically significant results, but also to matters of great practical importance as cancer is a leading cause of death in the world.

CHAPTER 5

Appendix

5.1. Nondimensionalization and Scaling Techniques

Many mathematical equations contain units, especially when physical quantities are concerned, but these units can make the equations more cumbersome to work with, and as a consequence it is often of great desire to remove all or some of the units from a problem.

Dynamical systems often involve many physical quantities, not just one or two, and so keeping track of them can be quite a challenge. This is why it is often advantageous to nondimensionalize a problem, as this can remove the units, make the problem simpler, and even reduce the number of parameters in the problem as will be shown in Example 33.

REMARK 32. *Nondimensionalization* is the full or partial removal of units from an equation involving physical quantities by a suitable substitution of variables.

There is no exact way to optimally nondimensionalize a problem, and as a result trial and error is often necessary to determine a suitable substitution. An outline of the procedure is provided below,

- (i) Identify all of the independent and dependent variables.
- (ii) Replace each of them with a quantity scaled relative to a characteristic unit of measure to be determined.
- (iii) Divide through by the coefficient of the highest order polynomial or derivative term.
- (iv) Determine a characteristic unit for each variable so that the coefficients of as many of the terms as possible becomes 1.

(v) Rewrite the system of equation in terms of their new dimensionless quantities.

EXAMPLE 33. Consider the model for the chemostat developed in [17],

$$(5.1.1) \quad \begin{aligned} \frac{dN}{dt} &= \left(\frac{k_{max}C}{k_n + C} \right) N - \frac{FN}{V} \\ \frac{dC}{dt} &= -\alpha \left(\frac{k_{max}C}{k_n + C} \right) N - \frac{FC}{V} + \frac{FC_0}{V} \end{aligned}$$

which has the six parameters $\alpha, k_{max}, k_n, F, V, C_0$, and where the variable N represents the bacterial population density and the variable C represents the nutrient concentration in the growth chamber.

Let $N = \bar{N}\hat{N}$, $C = \bar{C}\hat{C}$, and $t = \bar{t}\hat{t}$ where the variables \bar{N} , \bar{C} , and \bar{t} are scalar multiples and \hat{N} , \hat{C} , and \hat{t} represent the unit which carries the dimensions. Substituting these into (5.1.1) then yields,

$$\begin{aligned} \frac{d(\bar{N}\hat{N})}{d(\bar{t}\hat{t})} &= \left(\frac{k_{max}\bar{C}\hat{C}}{k_n + \bar{C}\hat{C}} \right) \bar{N}\hat{N} - \frac{F\bar{N}\hat{N}}{V} \\ \frac{d(\bar{C}\hat{C})}{d(\bar{t}\hat{t})} &= -\alpha \left(\frac{k_{max}\bar{C}\hat{C}}{k_n + \bar{C}\hat{C}} \right) \bar{N}\hat{N} - \frac{F\bar{C}\hat{C}}{V} + \frac{FC_0}{V}. \end{aligned}$$

Now we multiply both equations by τ and divide the first equation by \hat{N} and the second by \hat{C} which yields,

$$\begin{aligned} \frac{d\bar{N}}{d\bar{t}} &= \hat{t} \left(\frac{k_{max}\bar{C}\hat{C}}{k_n + \bar{C}\hat{C}} \right) \bar{N} - \frac{\hat{t}F\bar{N}}{V} \\ \frac{d\bar{C}}{d\bar{t}} &= -\alpha\hat{t} \left(\frac{k_{max}\bar{C}}{k_n + \bar{C}\hat{C}} \right) \bar{N}\hat{N} - \frac{\hat{t}F\bar{C}}{V} + \frac{\hat{t}FC_0}{V\hat{C}}. \end{aligned}$$

Let $\tau = \frac{V}{F}$ then,

$$\begin{aligned}\frac{d\bar{N}}{d\bar{t}} &= \hat{t} \left(\frac{k_{max}\bar{C}}{\frac{k_n}{\hat{C}} + \bar{C}} \right) \bar{N} - \bar{N} \\ \frac{d\bar{C}}{d\bar{t}} &= -\frac{\alpha\hat{t}}{\hat{C}} \left(\frac{k_{max}\bar{C}}{\frac{k_n}{\hat{C}} + \bar{C}} \right) \bar{N}\hat{N} - \bar{C} + \frac{C_0}{\hat{C}}.\end{aligned}$$

Let $k_n = \hat{C}$ then,

$$\begin{aligned}\frac{d\bar{N}}{d\bar{t}} &= \left(\frac{\hat{t}k_{max}\bar{C}}{1 + \bar{C}} \right) \bar{N} - \bar{N} \\ \frac{d\bar{C}}{d\bar{t}} &= -\frac{\alpha\hat{t}}{k_n} \left(\frac{k_{max}\bar{C}}{1 + \bar{C}} \right) \bar{N}\hat{N} - \bar{C} + \frac{C_0}{k_n}.\end{aligned}$$

Let $\hat{N} = \frac{k_n}{\alpha\tau k_{max}}$ thus,

$$\begin{aligned}\frac{d\bar{N}}{d\bar{t}} &= \left(\frac{\hat{t}k_{max}\bar{C}}{1 + \bar{C}} \right) \bar{N} - \bar{N} \\ \frac{d\bar{C}}{d\bar{t}} &= -\left(\frac{\bar{C}}{1 + \bar{C}} \right) \bar{N} - \bar{C} + \frac{C_0}{k_n}.\end{aligned}$$

For convenience let $N = \bar{N}$, $C = \bar{C}$, $\alpha_1 = \hat{t}k_{max}$, and $\alpha_2 = \frac{C_0}{k_n}$ thus,

$$\begin{aligned}\frac{dN}{d\bar{t}} &= \alpha_1 \left(\frac{C}{1 + C} \right) N - N \\ \frac{dC}{d\bar{t}} &= -\left(\frac{C}{1 + C} \right) N - C + \alpha_2\end{aligned}$$

which only contains two dimensionless parameters as opposed to the six we started with in (5.1.1). This not only makes the system less cumbersome, but helps to pinpoint exactly what parameters will qualitatively make the biggest difference when studying the behavior of the system.

5.2. Michaelis-Menten Kinetics

The following discussion comes from [20] and is used to help illustrate the Michaelis-Menten assumption used in (3.2.1). The growth rate of cells was modeled by Jacques Monod and has the same structure as the Michaelis-Menten enzyme kinetics. Suppose there is a cell which depends on a certain nutrient to survive or exist. Monod considered bacterial growth as a function of nutrient concentration and developed the following formula based on his experimental data for the specific growth rate,

$$\frac{dN}{Ndt} = \frac{rS}{a + S}$$

for constants $r > 0$ and $a > 0$. The constant r is the limiting value of the function, and when $t = a$ half saturation has been achieved. Since the growth rate and consumption rate are assumed to be proportional, $dN = -\gamma dS$, then the nutrient depletion is,

$$\frac{dS}{dt} = -\frac{1}{\gamma} \frac{rSN}{a + S}.$$

Consider the Michaelis-Menten part of (3.2.1) in the first equation which is,

$$\frac{dE}{dt} = \frac{p_1 E I_L}{g_1 + I_L}$$

where $p_1 = 0.1245$ and $g_1 = 2000$ when we neglect the other terms.

The specific growth rate is then,

$$(5.2.1) \quad f(I_L) = \frac{dE}{Edt} = \frac{p_1 I_L}{g_1 + I_L}$$

As an analogue to the above discussion we notice that in this case I_L is being considered as necessary to the growth of E . Although I_L is not a nutrient to E its presence acts to stimulate the production of E as though it were a nutrient. This is the main reason this type of function works to model the growth of these interacting cell populations. The graph of (5.2.1) is provided below in Figure 5.2.1.

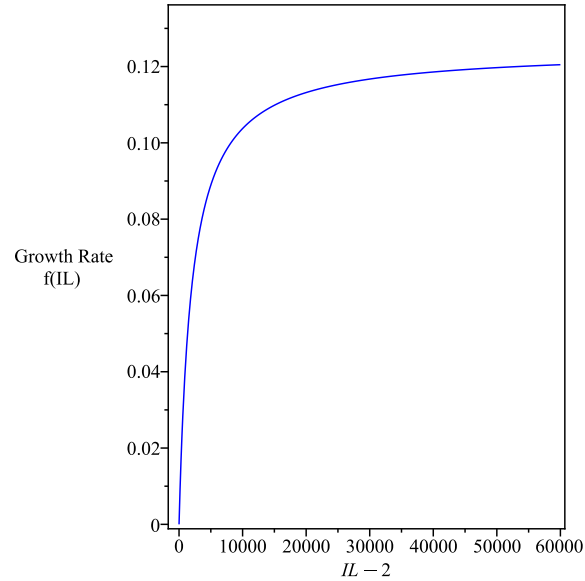


FIGURE 5.2.1. Plot of (5.2.1).

Notice that for large values of I_L the function tends to the parameter p_1 , and thus for large values of I_L we see the percentage of E that's being added to the model is $p_1 E$. This is observed algebraically by observing,

$$\lim_{I_L \rightarrow \infty} \frac{p_1 E I_L}{g_1 + I_L} = p_1 E$$

5.3. More about the Poincaré-Bendixson Theorem

The following theorem is used in Subsection 3.1.7, and provides a useful way to determine whether limit cycles exist in a planar dynamical system.

THEOREM 34 (Dulac-Bendixson Theorem). *Let $M(x_1, x_2)$ be a continuously differentiable function such that,*

$$\frac{\partial (M f_1)}{\partial x} + \frac{\partial (M f_2)}{\partial y}$$

has the same sign ($\neq 0$) in a set of measure zero in a simply connected region, then the planar autonomous dynamical system,

$$\begin{aligned}\frac{dx_1}{dt} &= f_1(x_1, x_2) \\ \frac{dx_2}{dt} &= f_2(x_1, x_2)\end{aligned}$$

has no closed orbits.

PROOF. Suppose there exists a function $M(x_1, x_2)$ such that,

$$\frac{\partial(Mf_1)}{\partial x_1} + \frac{\partial(Mf_2)}{\partial x_2} > 0$$

in a simply connected region S . Let Γ be a closed solution on the planar autonomous dynamical system in S , and let I be the interior of Γ . From Green's Theorem we obtain,

$$\begin{aligned}\int \int_I \left(\frac{\partial(Mf_1)}{\partial x_1} + \frac{\partial(Mf_2)}{\partial x_2} \right) dx_1 dx_2 &= \oint_{\Gamma} -Mf_2 dx_1 + Mf_1 dx_2 \\ &= \oint_{\Gamma} M(-x'_2 dx_1 + x'_1 dx_2),\end{aligned}$$

however on Γ we have that $dx_1 = x'_1 dt$ and $dx_2 = x'_2 dt$ and hence the integral evaluates to zero, which yields a contradiction and thus there can be no such closed solution Γ in S . \square

5.4. Elementary Bifurcations

We consider some of the most common bifurcation types below.

The simplest such equation which exhibits the saddle node bifurcation behavior is shown below,

$$(5.4.1) \quad x' = \mu - x^2$$

The solution set for the saddle node bifurcation is found by solving $x' = 0$ which yields $\bar{x} = \pm\sqrt{\mu}$. The stability of the system is determined by plotting the graph of (5.4.1) for the three cases where $\mu > 0$, $\mu < 0$, and $\mu = 0$. Doing this shows us that the system is stable when $\mu > 0$ and unstable for $\mu \leq 0$. This behavior has also been captured using XPPAut and is shown below in Figure 5.4.1.

The simplest such equation which exhibits the transcritical bifurcation behavior is shown below,

$$(5.4.2) \quad x' = \mu x - x^2.$$

The equilibrium points of (5.4.2) are $\bar{x}_0 = 0$ and $\bar{x}_1 = \mu$. Once stability is determined along each branch then using the fact that there are two lines in the (μ, x) plane we see that for $\mu < 0$ along the $x = 0$ branch the equilibrium points are stable, and for $\mu > 0$ along the same branch the equilibrium points are unstable. Along the $x = \mu$ branch the conclusions are reversed. This is shown in Figure 5.4.1 below.

The simplest such equation which exhibits the pitchfork bifurcation is shown below,

$$(5.4.3) \quad x' = \mu x - x^3.$$

The equilibrium points of (5.4.3) are $\bar{x}_0 = 0$ and $\bar{x}_{\pm} = \pm\sqrt{\mu}$. Differentiating (5.4.3) with respect to x yields -2μ when evaluated at \bar{x}_{\pm} and μ when evaluated at x_0 . Thus a bifurcation occurs at $(x, \mu) = (0, 0)$. By plotting (5.4.3) for the possible sign values of μ and considering the phase lines we can generate the bifurcation branches, which has been done in Figure 5.4.2 below.

The simplest such system which exhibits the Hopf-Bifurcation is shown below,

$$(5.4.4) \quad \begin{cases} x_1' = -x_2 + x_1(\mu - x_1^2 - x_2^2) \\ x_2' = x_1 + x_2(\mu - x_1^2 - x_2^2). \end{cases}$$

By letting $x_1 = r \cos(\theta)$ and $x_2 = r \sin(\theta)$ we can modify (5.4.4) into the form,

$$r' = r(\mu - r^2)$$

$$\theta' = 1.$$

This yields the equilibrium points $\bar{r}_0 = 0$ which corresponds to the steady state of $(0, 0)$ in (5.4.4) and $\bar{r}_{\pm} = \pm\sqrt{\mu}$ which corresponds to a periodic orbit of $x_1^2 + x_2^2 = \mu$ in (5.4.4). The bifurcation occurs at $(0, 0)$ and yields a supercritical bifurcation with two limit cycle branches appearing corresponding to \bar{r}_{\pm} . This behavior is captured below in Figure 5.4.2.

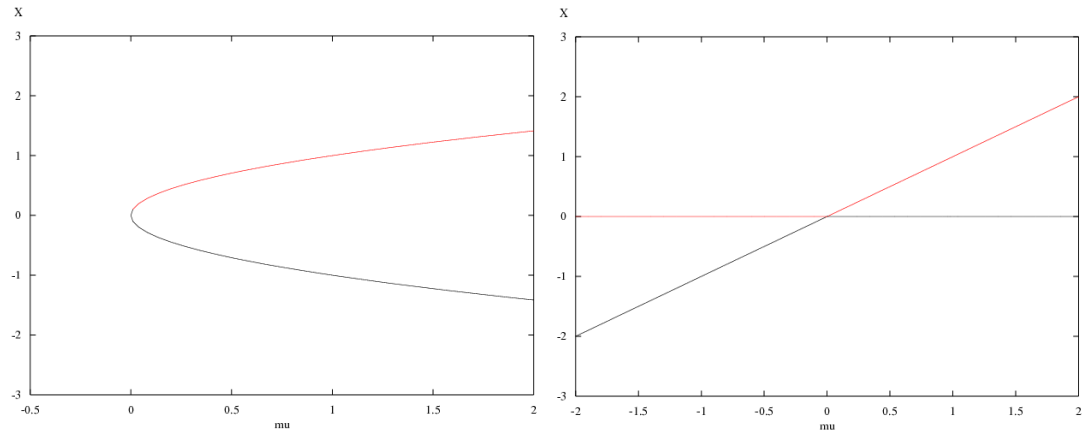


FIGURE 5.4.1. Left: Saddle Node Bifurcation. Right: Transcritical Bifurcation.

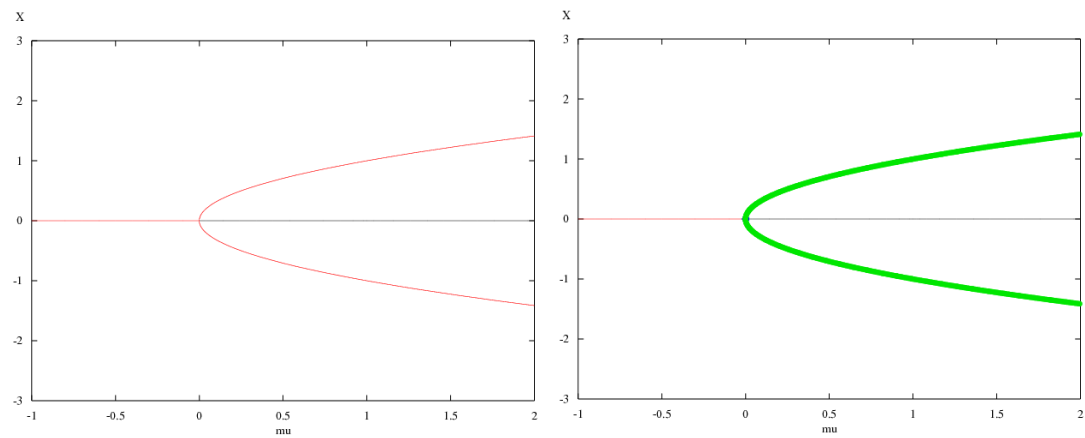


FIGURE 5.4.2. Left: Pitchfork Bifurcation. Right: Hopf-Bifurcation.

Bibliography

- [1] A. Abbas, A. Lichtman, and J. Pober, “Cellular and Molecular Immunology”, (1997)
- [2] J. Arciero, T. Jackson, and D. Kirschner, “A Mathematical Model of Tumor-Immune Evasion and siRNA Treatment”, (2004)
- [3] D. Armbuster, and E. Kostelich, “Introductory Differential Equations, From Linearity to Chaos”, (2005)
- [4] P. Blanchard, R. Devaney, and G. Hall, “Differential Equations”, (2006)
- [5] W. Boyce, and R. DiPrima, “Elementary Differential Equations and Boundary Value Problems 10th Edition”, (2012)
- [6] F. Brauer, and C. Castillo-Chavez, “Mathematical Models in Population Biology and Epidemiology”, (2001)
- [7] C. Cunningham, T. Jackson, and A. Usman, “Application of the Mathematical Model of Tumor-Immune Interactions for IL-2 Adoptive Immunotherapy to Studies on Patients with Metastatic Melanoma or Renal Cell Cancer”, (2005)
- [8] R. Devaney, M. Hirsch, and S. Smale, “Differential Equations, Dynamical Systems, and an Introduction to Chaos”, (2013)
- [9] L. Edelstein-Keshet, “Mathematical Models in Biology”, (2005)
- [10] M. Golubitsky, and D. Schaeffer, “Singularities and Groups in Bifurcation Theory, Volume I”, (1985)
- [11] J. Guckenheimer, and P. Holmes, “Nonlinear Oscillations, Dynamical Systems, and Bifurcations of Vector Fields”, (1983)
- [12] M. Hirsch, and S. Smale, “Differential Equations, Dynamical Systems, and Linear Algebra”, (1974)
- [13] D. Kirschner, and J. Panetta, “Modeling immunotherapy of the tumor - immune interaction”, (1997)
- [14] V. Kuznetsov, I. Makalkin, A. Perelson, and M. Taylor, “Nonlinear Dynamics of Immunogenic Tumors: Parameter Estimation and Global Bifurcation Analysis”, (1992)
- [15] S. Lovett, “Differential Geometry of Manifolds”, (2010)
- [16] J. Marsden, and M. McCracken, “The Hopf-Bifurcation and Its Applications”, (1976)
- [17] R. May, “Stability and Complexity in Model Ecosystems”, (1974)
- [18] L. Perko “Differential Equations and Dynamical Systems”, (1996)
- [19] H. Pollard, and M. Tenenbaum, “Ordinary Differential Equations”, (1963)
- [20] S. Rosenberg, S. Topalian, and J. Yang, et. al, “Treatment of 283 Consecutive Patients With Metastatic Melanoma or Renal Cell Cancer Using High-Dose Bolus Interleukin 2”, (1994)
- [21] H. Smith, “Modeling Microbial Populations in the Chemostat”, (2012)
- [22] G. Teschl, “Ordinary Differential Equations and Dynamical Systems”, (2013)
- [23] S. Wiggins, “Introduction to Applied Nonlinear Dynamical Systems and Chaos, 2nd Edition”, (2010)

Vita

Biographical Information

Author's Name: Joseph Albert Ferrara

Place of Birth:

Date of Birth:

Telephone:

Work Experience

August 2011 - August 2013 Graduate Teaching Assistant at UNF

April 2012 - present WyzAnt Tutor

Education

August 2011 - present Master of Science in Mathematical Sciences
University of North Florida, Jacksonville FL

Graduated May 2011 Bachelor of Science in Mathematics
University of North Florida, Jacksonville FL